Change in Geometry of a High Arctic glacier from 1948 to 2013 (Austre Lovénbreen, Svalbard)

Journal: *Geografiska Annaler: Series A, Physical Geography*

Manuscript ID: GAA1608-028.R1

Wiley - Manuscript type: Original Article

Date Submitted by the Author: n/a

Complete List of Authors:
MARLIN, Christelle; Université Pari-Sud 11, Earth Department; CNRS,
Tolle, Florian; Université de Franche-Comté - CNRS, Geography
Griselin, Madeleine; Université de Franche-Comté - CNRS, Geography
Bernard, Eric; Université de Franche-Comté - CNRS, Geography
Saintenoy, Albane; CNRS-GEOPS, ; Université de Paris-Sud 11 , Earth sciences
Quenet, Melanie; CNRS, ; Université de Paris-Sud 11 , Earth sciences
Friedt, Jean-Michel; Université de Franche-Comté - CNRS,

Keywords: glacier, mass balance, DEM

Abstract:

The change of Austre Lovénbreen (AL), a 4.5 km^2 land-based glacier along the west coast of Spitsbergen, is investigated using geodetic methods and mass balance measurements over 1948−2013. For 2008−2013, annual mass balances computed on 36-stake measurements were obtained, in addition to annual mass balances reconstructed from the neighbouring glaciers, Midtre Lovénbreen (1968−2007) and Austre Brøggerbreen (1963−1967). The mean rate of glacier retreat for 1948−2013 is −16.7 ± 0.3 m a^{-1}. Fluctuations in area (1948−2013 mean, −0.027 ± 0.002 km^2 a^{-1}) showed a slowing as the glacier recedes within its valley from 1990−1995. For 1962−2013, the average volume loss calculated by DEM subtraction of −0.441 ± 0.062 m w.e. a^{-1} (or −0.54 ± 0.07% a-1) is similar to the average annual mass balance (−0.451±0.007 m w.e. a^{-1}), demonstrating a good agreement between the loss rates computed by both methods over 1962−2013. When divided in two periods (1962−1995 and 1995−2013), an increase in the rate of ice mass loss is statistically significant for the glacier volume change. The 0°C isotherm elevation (based on mean May-September air temperatures) is estimated to have risen by about 250 m up to the upper parts of the glacier between 1948 and 2013. The glacier area exposed to melting during May to September almost increased by 1.8–fold while the area reduced by a third since 1948. Within a few years, the glacier area exposed to melting will decrease, leading the upper glacier parts under the 0°C isotherm while the snout will keep on retreating.

Abstract_final.docx

For publication in Geografiska Annaler, series A, Physical Geography

Corrected manuscript – 2016.

Change in Geometry of a High Arctic glacier from 1948 to 2013 (Austre Lovénbreen, Svalbard)

Christelle MARLIN[1*], Florian TOLLE[2], Madeleine GRISELIN[2], Eric BERNARD[2], Albane SAINTENOY[1], Mélanie QUENET[1] and Jean-Michel FRIEDT[3]

[1] Laboratoire GEOPS UMR 8148, Université Paris-Sud 11 - CNRS, Bât 504, 91405 Orsay Cedex, France
[2] Laboratoire ThéMA UMR 6049, Université de Bourgogne Franche-Comté - CNRS, 32 rue Mégevand, 25000 Besançon, France
[3] Laboratoire FEMTO-ST UMR 6174, Université de Bourgogne Franche-Comté - CNRS, Besançon, France

List of e-mail addresses:
Christelle Marlin: christelle.marlin@u-psud.fr
Florian Tolle: florian.tolle@univ-fcomte.fr
Madeleine Griselin: madeleine.griselin@univ-fcomte.fr
Eric Bernard: eric.bernard@univ-fcomte.fr
Albane Saintenoy: albane.saintenoy@u-psud.fr
Melanie Quenet: melanie.quenet@u-psud.fr
Jean-Michel Friedt: jean-michel.friedt@femto-st.fr

Key words
Glacier, mass balance, DEM, Austre Lovénbreen, Svalbard, Arctic
* *Corresponding author: christelle.marlin@u-psud.fr*

Abstract

The change of Austre Lovénbreen (AL), a 4.5 km^2 land-based glacier along the west coast of Spitsbergen, is investigated using geodetic methods and mass balance measurements over 1948–2013. For 2008−2013, annual mass balances computed on 36-stake measurements were obtained, in addition to annual mass balances reconstructed from the neighbouring glaciers, Midtre Lovénbreen (1968−2007) and Austre Brøggerbreen (1963−1967). The mean rate of glacier retreat for 1948–2013 is −16.7 ± 0.3 m a^{-1}. Fluctuations in area (1948–2013 mean, −0.027 ± 0.002 km^2 a^{-1}) showed a slowing as the glacier recedes within its valley from 1990−1995. For 1962–2013, the average volume loss calculated by DEM subtraction of −0.441 ± 0.062 m w.e. a^{-1} (or –0.54 ± 0.07% a^{-1}) is similar to the average annual mass balance (−0.451±0.007 m w.e. a^{-1}), demonstrating a good agreement between the loss rates computed by both methods over 1962−2013. When divided in two periods (1962−1995 and 1995−2013), an increase in the rate of ice mass loss is statistically significant for the glacier volume change. The 0°C isotherm elevation (based on mean May-September air temperatures) is estimated to have risen by about 250 m up to the upper parts of the glacier between 1948 and 2013. The glacier area exposed to melting during May to September almost increased by 1.8–fold while the area reduced by a third since 1948. Within a few years, the glacier area exposed to melting will decrease, leading the upper glacier parts under the 0°C isotherm while the snout will keep on retreating.

Introduction

As they are more sensitive to climate change, the small glaciers and ice caps currently contribute more to sea level rise than large ice sheets relative to their area (Paterson, 1994; Meier *et al.,* 2007; Gregory *et al.,* 2013; Stocker *et al*., 2013). To estimate the glacier contribution to sea water level requires data of mass balance or glacier geometry change (Dyurgerov *et al.,* 2010). In the Arctic, the dataset sources available to assess the long-term change of glaciers (in area and in volume) are quite rare, heterogeneous in nature and in accuracy, and available for a period not exceeding a century (Stocker *et al*., 2013). Among the methods used to investigate glacier geometry change, remote sensing methods provide information from the Arctic scale (e.g. Rignot and Kanagaratnam, 2006; Korona *et al.*, 2009) to the local scale (e.g. Rees and Arnold, 2007), with the largest sources of error at the largest scale. With 33,837 km^2 of ice caps and glaciers, Svalbard is among the largest glaciated areas in the High Arctic (Radić *et al*., 2013). It has the largest density of glaciers monitored in the Arctic island zone defined by the World Glacier Monitoring Service (WGMS, 2016). Along the west coast of Spitsbergen, the Brøgger Peninsula displays several small valley glaciers among which Midtre Lovénbreen (ML), Austre Lovénbreen (AL) and Austre Brøggerbreen (AB) have been studied since the 1960s (Corbel, 1966; Corbel, 1970; Hagen and Liestøl, 1990; Liestøl, 1993; **WGMS**, 2016). Recently, the investigations on these valley glaciers have been intensified (e.g. Rippin *et al.*, 2003; Kohler *et al*., 2007; Rees and Arnold, 2007; Murray *et al.*, 2007; Mingxing *et al.*, 2010; Barrand *et al.*, 2010; James *et al.*, 2012). Most of these authors have shown a constant but irregular retreat of these glacier fronts since the end of the Little Ice Age (LIA).

The present paper investigates the changes in length, surface and volume of AL (78.87°N, 12.15°E) over a long period (1948−2013), using measurements of front position and annual mass balance combined to several dataset sources: a digitized contour map, aerial photographs, satellite images and digital elevation models (DEMs). In addition, the Ny-Ålesund station (6 km west of the study area) provides climate data from 1969. By taking into account a catchment area constant since the LIA, we discuss the potential relation between the glacier geometry change (area, volume) and air temperature data. The long-term evolution is discussed, combining our mass balances obtained on the AL with those extrapolated from ML and AB following the observed close correlations with these two neighbouring glaciers. The paper also provides a discussion about consistency of methods used for assessing volume change of AL over 1962−2013. Then, in order to understand the ongoing shrinking rates, the evolution of the average 0°C isotherm over May–September is proposed and examined for 7 dates between 1948 and 2013.

1. General settings

Svalbard, an archipelago with 55.5% glacier cover, represents about 10% of the total Arctic small glaciers area (Liestøl, 1993; Kohler *et al.*, 2007; Radić *et al.*, 2013). Similar to what is observed throughout the Arctic, this area is very reactive to climate change: Hagen *et al.* (2003) stated that all the small glaciers (area lower than 10 km^2) have been clearly retreating since the end of the LIA. Small valley glaciers of the Brøgger Peninsula have thus lost both in mass and in area (Lefauconnier and Hagen, 1990; Hagen *et al.*, 1993; Liestøl, 1993; Lefauconnier *et al.*, 1999; Kohler *et al.*, 2007). In a recent study, Kohler *et al.* (2007) demonstrated that the average thinning rate of ML has increased steadily since 1936. They showed that the thinning rates from 2003 to 2005 were more than four times the average of the first period (1936–1962).

Regarding its climate, the Brøgger Peninsula is subject to the influence of the northern extremity of the warm North Atlantic current (Liestøl, 1993). The climate at Ny-Ålesund (8 m above sea level or m a.s.l.) is of polar oceanic type with a mean annual air temperature (MAAT) of −5.2°C and a total annual precipitation of 427 mm water equivalent (w.e.) for 1981−2010 (Førland *et al.*, 2011). Over an earlier period (1961−1990), these parameters (Ny-Ålesund data for 1975−1990 and interpolated from Longyearbyen data before 1975) were lower (−6.3°C for air temperature and 385 mm for precipitation), indicating that a significant climate change occurred over the last few decades (Førland *et al.*, 2011).

The AL glacier is a small land-based valley glacier, 4 km long from South to North along the Brøgger Peninsula (Figure 1). The glacier area was 4.48 km^2 in 2013 and its elevation ranges from 50 to 550 m a.s.l. Its catchment area spreads over 10.577 km^2, taking into account an outlet where the main stream crosses a compact calcareous outcrop 400 m upstream from the coastline (Figure 1). The catchment is characterized by a proglacial area downstream and the glacier it-self upstream, surrounded by a series of rugged mountain peaks whose elevation reaches 880 m a.s.l. (Nobilefjellet). The first glaciological and hydrological investigations in the

Brøgger Peninsula were conducted by French scientists during the early 1960s on the Lovén glaciers. In 1965, Geoffray (1968) implemented a network of 17 stakes on AL. Preliminary hydro-glaciological investigations conducted by Vivian (1964) were pursued by Vincent and Geoffray (1970). Two decades later, Griselin (1982; 1985) proposed the first hydrological balance of the AL catchment. More recently Mingxing *et al.* (2010) published annual mass balance data for 2005–2006.

2. Data and methods

The techniques of airborne and satellite remote sensing combined with topographic data imported into a GIS database are relevant tools to investigate geometry changes of glaciers (Haakensen, 1986; Rippin *et al.*, 2003; Kohler *et al.*, 2007; Rees and Arnold, 2007; Moholdt *et al.*, 2010; Friedt *et al.*, 2012). In addition, field measurements (GPS, snow drills, ice stake measurements, ground penetrating radar [GPR]) are common complements to remote sensing techniques (Østrem and Brugman, 1991; Hock, 2005; Brandt and Kohler, 2006; Mingxing *et al.*, 2010; Saintenoy *et al.*, 2013).

In the present paper, the change in AL geometry over the 1948–2013 period is investigated using (i) geodetic methods (a topographic map, aerial photos, satellite images, GPS tracks, airborne light detection and ranging [LIDAR]) and (ii) annual mass balance (*B*a after Cogley *et al.,* [2011]) measured from 2008 to 2015. The source materials and data vary depending on whether the glacier change is studied in terms of length, area or volume change (Figure 2a–f).

2.1 Front position and area change

- *1962–1965 German topographic map* – East German scientists produced a 1/25,000 map from 1962 to 1965 (Pillewizer, 1967) that we georeferenced (Figure 2a). In this paper, this dataset will be referred to as the "1962–1965 map" since the AL snout (elevation lower than 300 m a.s.l.) was mapped in 1962 and the higher part of the glacier (above 300 m a.s.l.) was mapped in 1965.
- *Aerial photos* – Six aerial stereographic photographs (Figure 2b) provided by the Norsk Polarinstitutt (NPI) were used to determine the glacier front position at different dates: 1948 (unknown scale), 1966 (scale of 1/50,000), 1971 (1/20,000 and 1/6,000), 1977 (1/50,000), 1990 (1/50,000 and 1/15,000) and 1995 (1/15,000). We georeferenced original aerial images with a GPS-referenced ground control points (GCP), at a density of approximately 1 point per km^2 using relevant ground features on the surrounding ridges and in the glacier forefield.
- *Airborne and satellite data* – For the period 1995 to 2008, the only available, dataset at high resolution was a 2005 Scott Polar Institute Airborne LIDAR DEM (Rees and Arnold, 2007). In this paper, it was only used to outline the front position in 2005 since the survey only covers AL glacier forefield and snout. A Formosat-2 image was used for 2009 (Friedt *et al.*, 2012). Before 2006, multiple georeferenced Landsat7 images are available on the USGS website. Seven images (1985, 1989, 1990, 1998, 1999, 2002 and 2006) were

analysed but rejected due to a poor pixel definition (30 m x 30 m). Additionally, on these Landsat7 images, we found the differentiation between the ice or snow-covered surfaces from rock or morainic material challenging, leading to an error of ±100 m on the glacier front positioning.

- *Front positioning by GPS* – For the 2008–2013 period, the glacier front limit was surveyed every year at the end of September with a Coarse Acquisition GPS. When Formosat-2 images and GPS data were available for the same year, *in situ* GPS front positioning is considered more accurate.

Thus, a total of 14 AL front positions can be investigated over 1948–2013. The front positions were manually delineated for years between 1948 and 2005. After 2005, i.e for 2008–2013, the snout positions were determined by GPS. Since the margin is covered with rock debris and some residual ice may remain in the proglacial moraine, the actual glacier front is not always easy to delineate neither on images nor in the field. Even if the limit may also have changed in the upper part of the glacier, the available source materials are not precise enough to determine accurately any significant difference on the upper parts of the glacier (Bernard *et al.*, 2014). This is due to (i) the steepness of surrounding slopes and/or (ii) the snow cover at the foot of slopes covering the rimaye (Bernard *et al.*, 2013). We therefore used a single image as the reference to delineate the glacier area behind the snout (Formosat-2 image of summer 2009).

In a previous publication by our group, Friedt *et al.* (2012) analysed the error margin on the AL glacier limit position. Their results are consistent with the uncertainty analysis published by Rippin *et al.* (2003). As we used the same dataset sources as Friedt *et al.* (2012), the uncertainty analysis made in the paper remains valid here:

- the contour map and all airborne/satellite images were re-sampled on a 5 m x 5 m grid;
- The glacier boundary analysis using manual colour identification (upper limit of the glacier for all years and snout position before 2008) yields a 2 pixel uncertainty, i.e. an uncertainty of ± 10m;
- GPS delineation of the snout (2008–2013) yields a horizontal uncertainty of ±5 m.

Such boundary position uncertainties yield a variable uncertainty on the glacier area (Table 1): considering that the glacier limit is largely constant upstream (our reference for all years being the 2009 glacier ice-rock interface; see yellow, thick line on Figure 3) and that only the snout position is significantly evolving (see the length of glacier front in Table 1 and Figure 3), the area uncertainty is given by the sum of (i) the uncertainty on the upper glacier limit (length if 12.93 km times 10 m for all years) and (ii) the uncertainty on the independently measured snout position (the length of the front times 10 m for 1948–2005 or times 5 m for 2008–2013)

2.2 Volume change

In order to assess the volume change of the glacier over 1962–2013 (51 years), we compared different dataset resources available for AL, all converted into DEMs: (i) the "1962–1965 map" (ii) the 1995 DEM (NPI) and (iii) two new DEMs produced from our GPS measurements in 2009 and

2013.

Other sources exist but, based on the elevation uncertainty analysis, only datasets exhibiting sub-meter standard deviation on the altitude were considered. Most significantly, we rejected:

- the 2007 SPIRIT-derived DEM (SPOT5 stereoscopic survey of Polar Ice provided by CNES-France in the frame of 2007-2009 IPY) due to a large elevation uncertainty (Korona *et al*., 2009);
- the 2006 DEM mentioned in Friedt *et al.* (2012) due to a poor coverage of some of the key areas of the catchment;
- the 2005 Scott Polar Institute DEM derived from a LIDAR survey (Rees and Arnold, 2007) which has 0.15 m vertical accuracy but only covering part of the studied catchment (the glacier forefield and the snout).

Hence, the three periods investigated herein for assessing the volume change are 1962–1995, 1995–2009 and 2009–2013 (Figure 2):

- *1962–1965 German topographic map* (Figure 2a; Pillewizer, 1967) – Original 20 m contour line intervals were manually delineated in a vector format. Based on this linear elevation information, interpolation was performed to obtain a continuous DEM of the glacier surface. The elevation error was estimated by Friedt *et al.* (2012) by analysing DEM errors (mean and standard deviation) in areas of the proglacial moraine known to be static over time: the resulting standard deviation was stated as 3 m. Cartographical approximations on the original map and computation artefacts were the source of cumulative errors (Friedt *et al.,* 2012).

- *1995 DEM* (Figure 2c) – This DEM provided by the NPI was derived using analytical photogrammetry from six stereo-overlapping aerial photographs taken in August 1995 (Rippin *et al.*, 2003; Kohler *et al.*, 2007). According to Kohler *et al.* (2007) and Aas F. (personal communication), the DEM of 1995 has an elevation uncertainty within ±1.5 m.
- *2009 DEM and 2013 DEM* (Figure 2d) – Both DEM were made by snowmobile carrying a dual-frequency GPS (Trimble Geo XH, Zephyr antenna) in order to obtain the glacier surface elevation in April 2010 and April 2014. The resulting dataset was post-processed for electromagnetic delay correction using reference Rinex correction files provided by the geodetic station located in Ny-Ålesund. Snow thickness interpolated from *in-situ* measurements (avalanche probe and PICO [University of Nebraska, Lincoln, USA] snow drill) made in April 2010 and 2014 was removed from the glacier surface elevation of April in order to provide the glacier elevation at the end of the 2009 and 2013 summers. These GPS derived elevation models exhibit a standard deviation on the elevation of 0.5 m, including both measurement uncertainty and experimental procedure related uncertainties.

When subtracting two DEMs, the uncertainty of elevation is assumed to be equal to the sum of elevation uncertainty of each image or map. It is therefore within ±4.5 m between the “1962-1965 map” and 1995 photogrammetry-derived DEM, within ±2.0 m uncertainty between the 1995 DEM and a GPS-derived DEM, within ±1.0 m uncertainty between two

GPS-derived DEMs and within ±3.5 m uncertainty between the "1962-1965 map" and a GPS-derived DEM. The uncertainty on volume change is therefore the uncertainty of elevation times the mean glacier areas between two years.

2.3 Mass balance

Field measurements of ablation and accumulation have been made yearly using a 36-stake network that we set up in 2007 to cover the whole AL glacier surface (Figure 2e). Glacier-wide mass balance is computed from measurements conducted twice a year: at the end of winter (late April / early May) for winter mass balance (not used in this paper) and at the end of summer (late September /early October) for annual mass balance (*B*a; after Cogley *et al*., 2011). The *B*a were computed for 8 years (from 2008 to 2015 meaning glaciological years 2007–2008 to 2014–2015). The AL *B*a was obtained by inverse distance weighting interpolation of 36-stake measurements (Bernard *et al.*, 2009; Bernard, 2011).

All height measurements at stakes are independent and the uncertainty on the height measurement is estimated to be ± 0.05 m. Thus, the uncertainty on *B*a derived from subtracting independently measured stake heights is ±0.10 m or ±0.09 m water equivalent (mean ice density of 0.9; e.g. Moholdt *et al.*, 2010). This uncertainty considered on *B*a is consistent with that given by Fountain and Vecchia (1999) for a glacier mass balance computed with about 30 stakes. The uncertainty of *B*a averaged over a time period (year i–year j) is therefore the sum of the *B*a uncertainty of each year (year i and year j) divided by the number of years separating the years i and j.

In addition, previous stake measurements for 1965–1975 were obtained once in 1975 by Brossard and Joly (1986) at 7-stakes retrieved on the snout from the 17-stake network installed in 1965 (Geoffray, 1968), (Figure 2f).

The longest *B*a time series in the Brøgger peninsula concern two other glaciers: (i) ML, the neighbouring glacier of AL and (ii) AB, 6 km further West (Figure 1). In this paper, we use the *B*a of ML between 1968 and 2007 provided by WGMS (2016). The ML *B*a were computed by averaging 10-stake measurements within 100 m elevation bins along the central line (Barrand *et al*., 2010). For 1963−1967, we used the AB *B*a data given by Lefauconnier and Hagen (1990). Before 1967, these authors estimated AB *B*a from positive air temperature of July to September recorded at Longyearbyen combined to winter precipitation for which coefficient correlation is 0.90).

2.4 Air temperature

Air temperature (AT) time series are recorded since 1969 at the Ny-Ålesund station at 8 m a.s.l. (eKlima, 2013). The AT over AL was deduced by applying an altitude−AT gradient to the Ny-Ålesund AT data. The gradient was established from daily AT obtained from two temperature loggers (Hobo pro V2 U23-004 Onset Hobo data loggers, Bourne, MA, USA; accuracy of ±0.2°C) installed on the AL: one downstream at 148 m a.s.l and the other upstream at 481 m a.s.l. The resulting average altitude−AT (−0.005°C m^{-1} for May-September) is consistent with the literature (e.g. Corbel, 1966; Geoffray, 1968; Corbel, 1970; Griselin, 1982 and Griselin and Marlin, 1999 for AL; Joly, 1994 for ML). Additionally, a third similar temperature logger was set in the AL proglacial moraine at 25 m a.s.l.: the mean annual difference of 0.007°C lower than the accuracy on temperature measurement, indicates that no significant longitudinal gradient exists between Ny-Ålesund and the AL catchment, 6 km further East.

3. Results

3.1 AT data

In this paper, we consider hydro-glaciological years from October 1 to September 30 in order to compare AT data with *B*a that is measured at the end of September/beginning of October each year. Over 1970–2013 (meaning glaciological years from 1969−1970 to 2012−2013), the MAAT in Ny-Ålesund was −5.22°C (standard deviation [SD] of 1.27°C). Over the period, the MAAT displays a positive temporal trend of +0.57°C/decade (Figure 4). This is in agreement with the data analysed by Førland *et al.* (2011) for Svalbard. The segmented linear regression technique explained by Oosterbaan (1994) was applied to find potential breakpoints in the MAAT time series. The result is the following: the MAAT time series is statistically analysed as a period of constant temperature followed by a period of uniform temperature increase with a breakpoint between 1994 and 1995 (98% confidence interval): this temperature change occurring in the mid-1990s may be relevant to understand glacier volume evolution. During the first 25 years (1970−1994), there is no clear temporal trend (+0.04°C per decade) as opposed to the following 19 years (1995–2013) for which the MAAT significantly increases with a trend of +1.38°C/decade. This 1995–2013 gradient is 2.4 times the average gradient calculated over the whole period (1970–2013). The MAAT value is −4.45°C (SD of 1.12°C) over 1995–2013.

Mean summer air temperature (MSAT) was also calculated for May to September as an indicator of the melting period at Ny-Ålesund: it was +1.88°C (SD of 0.71°C) for 1970–2013. Using the segmented linear regression technique (Oosterbaan, 1994), the MSAT may be also separated into 2 periods with a statistically significant breakpoint between 1996 and 1997: the trend over 1970–2013 was +0.34°C/decade (trends of +0.10°C/decade for 1970–1996 and +0.90°C/decade for 1997–2013; Figure 4). The mean MSAT value was +1.57°C (SD of 0.59°C) for 1970–1996 and increased to +2.37°C (SD of 0.59°C) for 1997–2013 (Figure 4).

3.2 AL length change

Between 1948 and 2013, AL front showed clear changes (Figure 3). The recession was not however equally distributed over the front (Figure 3). A maximum retreat distance may be estimated along the central flow line with a total recession of 1 247 ± 20 m between 1948 and 2013, i.e. a mean retreat rate of −19.2 ± 0.3 m a^{-1} (Table 1). Seven fanned out profiles (Figure 3) were arbitrarily yet regularly selected to assess the variability of the glacier retreat due to irregularities in the underlying bedrock. The results indicate a mean retreat rate of −16.7 ± 0.3 m a^{-1} between 1948 and 2013 with rate ranges from −12.8 ± 0.3 m a^{-1} on the western part to −19.2 ± 0.3 m a^{-1} in the central axis (Table 1; Figure 3). Figure 5a shows a regular retreat, linear with time, for the average of the seven fanned out profiles whereas an increase of the retreat rate from 2005 is noticeable for the central one. The retreat rate range is consistent with that indicated for the central line of Midtre Lovénbreen, i.e. −15 m a^{-1} (Hansen, 1999). Even if investigated over a short period (1-year interval), Mingxing *et al.* (2010) mentioned a similar value for the mean annual AL retreat rate (−21.8 m a^{-1} for 2005–2006).

In details, the annual retreat rate displayed a wide range of values (Table 1). Mingxing *et al.* (2010) also mentioned great differences in the AL retreat rates along the central glacier flowline (from −2.8 m a^{-1} to −77.3 m a^{-1} for 2005–2006).

The important spatio-temporal variability is mostly linked to differences in ice thickness and in bedrock morphology. Moreover glacier length change is partly compensated for by glacier flow (Vincent *et al*., 2000). Mingxing *et al.* (2010) measured the surface ice flow velocity of AL using differential GPS, they obtained a mean velocity of 2.5 m a^{-1} along the central line of the AL snout, consistent with a velocity of 4 m a^{-1} given by Rees and Arnold (2007) for 2003−2005 for the ML also along the central line. The velocity is at least five times lower than the glacier margin retreat rate.

3.3 AL area change

In this paper, the change in area (Table 1 and Figure 5b) only shows the reduction of the snout area since the same upper limit of the glacier (measured in 2009) was considered constant for all years. Therefore, the glacier area is likely to be underestimated before 2009 and slightly overestimated after 2009. The results obtained for the area change of AL indicate that in 2013 the glacier covered 71% of its 1948 area. In other words, in 2013, the glacier covered only 42% of the total basin area (10.577 km^2), whereas it occupied 60% of the catchment in the late 1940s.

The glacier area data plotted over time in Figure 5b indicates a progressive temporal decrease (fit resulting from minimizing quadratic error) with an average reduction rate over 1948−2013, similarly to 1962−2013 Table 2). An uncertainty of ±0.002 km^2 a^{-1} is obtained on the slope by computing the uncertainty on the slope of the regression “glacier area upon time”, which is the SD of the slope times a variable following Student's distribution for a 95% confidence interval (Oosterbaan, 1994). The uncertainty is less than 10% of the observed temporal trend.

Figure 5b shows that the area change with time has two periods of regular decrease separated by a perceptible breakpoint between 1990 and 1995: the gradient decreased from −0.033 ± 0.003 km^2 a^{-1} for 1948−1995 (similar to −0.032 ± 0.003 km^2 for 1962−1995) to −0.018 ± 0.005 km^2 a^{-1} for 1995−2013 (Table 2).

3.4 AL volume change determined by DEM differences

The AL change in volume was estimated by subtracting two by two four DEMs covering the 1962−2013 period that we can separate into three sub-periods: 1962−1995, 1995−2009, 2009−2013 (Figure 6 and Table 2). For the whole 1962−2013 period, the total glacier ice volume loss, was estimated at 129.1 ± 18.1 x 10^6 m^3 (Table 2). This corresponds to an average reduction rate of −2.5 ± 0.4 x 10^6 m^3 a^{-1} (the ratio of the volume divided by 51 years) or an average elevation difference of −0.490 ± 0.069 m a^{-1} (ratio of −2.5 x 10^6 m^3 a^{-1} by the average glacier area between 1962 and 2013 (5.17 km^2).

The annual volume change rate is not constant between the three investigated periods:

- −2.3 ± 0.7 x 10^6 m^3 a^{-1} (1962−1995).The average elevation difference was −0.427 ± 0.136 m a^{-1} (based on the average 1962−1995 glacier area, 5.32 km^2);
- −3.4 ± 0.7 x 10^6 m^3 a^{-1} (1995−2009). In terms of elevation difference, the rate was −0.720 ± 0.143 m a^{-1} based on an average 1995−2009 glacier area (4.67 km^2);
- −1.8 ± 1.1 x 10^6 m^3 a^{-1} (2009−2013). Expressed as elevation difference, the rate was −0.394 ± 0.250 m a^{-1} based on an average 2009−2013 glacier area (4.51 km^2).

For this last period, we see that the uncertainty accounts for two third of the calculated net ice loss. As already shown by Friedt *et al.* (2012), a four−year interval is clearly too short to accurately determine the glacier volume change but only the DEMs of 2009 and 2013 were surveyed with the same instrument (GPS) and methods, in the frame of this study. To reduce the uncertainties, the two last periods (1995−2009 and 2009−2013) were gathered and gave a net ice loss of −3.0 ± 0.5 x 10^6 m^3 a^{-1} for the whole period. Expressed as elevation difference, the rate was −0.649 ± 0.111 m a^{-1} with respect to an average 1995−2013 glacier area (4.64 km^2).

Using a mean ice density of 0.9 (e.g. Moholdt *et al.*, 2010), AL lost −2.3 ± 0.3 x 10^6 m^3 a^{-1} water equivalent (w.e) during 1962–2013. The loss was –2.0 ± 0.7 and −2.7 ± 0.5 x 10^6 m^3 a^{-1} w.e. for 1962–1995 and 1995–2013 respectively (Table 2).

3.5 AL mass balance

The AL *B*a was measured yearly for 2008–2015 (Figure 7; Table 3). The average *B*a was −0.421 ± 0.030 m w.e. a^{-1} for 2008–2015. The high SD (0.439 m w.e. a^{-1}) reflected a high interannual variability of *B*a. With the exception of 2014, all *B*a were negative with considerable contrasts between years: from +0.010 ± 0.090 m w.e. (2014) to −1.111 ± 0.090 m w.e. (2013). The accumulation area ratio (AAR after Dyurgerov *et al*., (2009); AAR is calculated as the accumulation area/total glacier area ratio) ranged from 0.00 to 0.66 over 2008–2015.

Earlier studies of the AL catchment (Geoffray, 1968; Griselin, 1982) did not provide data to establish past *B*a since the 7 available data were located in the ablation area only. Between 1965 and 1975 the point mass balance (*b*a) of the partial Geoffray's stake network spatially ranged from −1.05 m a^{-1} downstream to −0.24 m a^{-1} upstream (Table 4; Brossard and Joly, 1986). They fall within the same range as the 1962−1995 DEM subtraction at these same 7 points (from −0.17 to −1.09 m a^{-1}; Table 4).

So, in order to estimate the past AL *B*a for 1967−2007, we correlated AL *versus* ML *B*a data, both series having 8 years in common (2008 to 2015). We obtained a strong correlation between the *B*a series for 2008−2015, with a linear fit yielding the following equation (Figure 8a):

*B*a(AL) = 1.136 x *B*a(ML) − 0.014 (n = 8; r = 0.992) Equation 1

where *B*a were given in m w.e.

By applying Equation 1 to the series of ML *B*a, we obtained an AL *B*a time series extrapolated for 1968−2007 (Figure 7). Since *B*a were not available for ML prior to 1968, we used the estimated *B*a values computed by Lefauconnier and Hagen (1990) for AB. Subsequently, the strong correlation between AB and ML (Equation 2; Figure 8b) enabled AL *B*a series to be calculated for 1963−1967 (Figure 7) using again Equation 1 between AL and ML.

$Ba(ML) = 0.9959 \times Ba(AB) + 0.069$ (n = 21; r = 0.994) Equation 2

where *B*a are given in m w.e.

For extrapolated AL *B*a, error bars are driven by the ML error bar (± 0.25 m according to Kohler *et al.*, 2007) times the regression coefficient, with uncertainty on each regression coefficient bringing a negligible contribution since r is close to 1 (see the equations in Oosterbaan, 1994). Hence, we assessed uncertainties of ±0.26 m w.e. for each AL extrapolated *B*a between 1968 and 2007 and ±0.28 m w.e. between 1963 and 1967 (95% confidence interval).

The average 1963−2013 *B*a was −0.451 ± 0.007 m w.e. a^{-1} with −0.422 ± 0.016 m w.e. a^{-1} for 1963−1995 and −0.505 ± 0.020 m w.e. a^{-1} for 1996−2013 (Table 2). The whole AL *B*a time series (1963−2013) showed a negligible increase in the temporal trend of −0.0026 m w.e. a^{-1}. We observed that very negative *B*a of AL such as in 2011 or 2013 (more than twice the average *B*a) were not exceptional since they occurred 8 times during 1963–2015 (Figure 7).

4. Discussion

During the 1948−2013 period, AL underwent changes of geometry (length, area and volume). The following discussion addresses (i) the change rates through time, (ii) the differences between the methods to estimate the change in volume (*B*a *versus* DEM) and (iii) the relationship between geometry change and evolution of glacier areas exposed to melting.

4.1 Variations in rate of AL retreat (length, area) for 1948–2013

Whatever the resource type used to estimate the glacier retreat in length or in area through time (Figures 5a and 5b), we observed a strong linear fit. However, it was not possible to assess the changes in glacier higher in the catchment for reasons explained in section 2.1.

The mean retreat calculated by averaging the length along 7 profiles was relatively constant in time (Figure 3). A straight line with a mean slope of −16.7 ± 0.3 m a^{-1} (n = 14 and r = 1.000) is representative of the average retreat rate of the glacier terminus. It is notable that the average AL velocity (2.5 m a^{-1} according to Mingxing *et al.*, 2010) does not exceed the average front retreat rate along the main flow line which is quite homogeneous over 1948−2013 (−19.2 ± 0.3 m a^{-1}; n = 14 and r = 0.997).

On the retreat rate *versus* time relationship determined for the central line (Figure 5a), the breakpoint in 2005 is not the consequence of a climatic change but illustrates the local predominance of the surrounding terrain topography in the apparent acceleration of the axial retreat. Averaging over 7 profiles smooths out bedrock topographic features and yields a homogeneous retreat rate rather constant in time.

Regarding the glacier area, the average change was −0.027 ± 0.002 km^2 a^{-1} over 1948–2013 (n=14 and r = 0.993). A slowdown in the area reduction was observed between 1990 and 1995 (Figure 5b). This breakpoint may be surprising when considering the MAAT or MSAT series (Figure 4): the AT gradient increased after 1994, whereas the reduction rate of the glacier area slowed down. This apparent divergence may be partially explained by the reduction of the glacier terminus exposed to melting. We can observe that, in 1948, the glacier terminus was widely spread out in the glacier forefield uphill the LIA terminal moraine (Figure 3). Compared to 2013, the glacier terminus was less thick and the front itself was rather flat because it was not constrained by the surrounding terrain (Figure 9). In the present-day configuration, the glacier snout clearly is constrained on its eastern and western sides by the steep slopes of the glacier basin valley. The glacier snout gradually became thicker and its front steeper over time (Figure 9). If we compare the ice thicknesses at the glacier snout at a same distance from the respective fronts of 1962, 1995, 2009 and 2013, we highlight the increasing values of ice thickness: 35, 45, 72 and 76 m at 500 m and 70, 116, 123 and 124 m at 1000 m from the front of 1962, 1995, 2009 and 2013 respectively. Further discussion about the glacier areas exposed to melting is given below in section 4.5.

Even if the changes of snout length as well as glacier area are two convenient, visible proxies to study glacier dynamics, they may be delicate to interpret since they combine several processes that are not only dependent on climate conditions. Glacier shrinkage is also related to parameters including ice thickness, glacier velocity, basal thermal state of glacier, topography and roughness of underlying bedrock and geological structures (slope, fractures). Therefore, to assess glacier changes, glaciological investigations have to focus on volume in addition area or length of glaciers.

4.2 Variation in volume (reduction rate and percentage of total AL volume) for 1962–2013

Regarding the methods for assessing the volume change of the glacier, it could be hazardous to compare heterogeneous sources of dataset since investigating the long term change of glacier often requires the use of various documents (maps, aerial photos, satellite and airborne images) with different accuracies and scales. In the case of AL, great care was applied to minimize data artefacts but oldest sources showed some discrepancies from expected trends. For the 2009 and 2013 datasets, the DEM difference produced by Rinex-post-processed GPS measurements is expected to lead to the best accuracy of our datasets but such a short time interval actually yields unacceptable signal to noise ratio (64%, i.e. an error of 0.25 m a^{-1} for a value of −0.39 m a^{-1}). This short time interval will hence not be considered, in favor of the longer time interval 1995−2013 over which uncertainties are reduced to yield an acceptable signal to noise ratio of at least 10.

Like for the AL area change, the results undoubtedly indicate that AL reduced in volume over 1962−2013 with a rate of −2.5 ± 0.3 x 10^6 m^3 a^{-1} of ice for an average elevation difference of −0.490 ± 0.069 m a^{-1} (Table 2).

Using the 2009 glacier volume (349 ± 41 x 10^6 m^3) obtained by Saintenoy *et al.* (2013), we can estimate the glacier volume in 1962 by adding ice loss between 1962 and 2009 (122 ± 33 x 10^6 m^3): the glacier volume was 471 ± 74 x 10^6 m^3 in 1962). Regarding the 1962–2013 ice loss (129.1 ± 18.1 x 10^6 m^3), it therefore represents a high proportion (27.4 ± 3.8%) of the 1962 glacier volume. AL lost −0.54 ± 0.07% per year of its volume over 1962−2013.

However, the loss rate was not constant through time and displayed a noticeable acceleration of 30% between 1962−1995 and 1995−2013 (−0.384 ±0.123 m w.e. a^{-1} for 1962−1995 *versus* −0.584 ±0.100 m w.e. a^{-1} for 1995−2013; Figure 7 and Figure 10; Table 2). However, the acceleration is better demonstrated with *B*a data because the error bars are lower than the ones on DEM differences. This acceleration is much lower than that given by Kohler *et al.* (2007) for ML (+245% between 1962−1969 and 2003−2005), which was computed on short time-spans instead of continuous, long time series to characterize the changes (1936−2005).

Expressed as change with respect to the whole glacier volume, the glacier lost 16 ± 5% of its 1962 volume at an average loss rate of −0.48 ± 0.15% a^{-1} during the first 33-year period while the glacier lost 14 ± 2% of its 1995 volume at a rate of –0.76 ± 0.13% a^{-1} during the following 18-year period.

However, the acceleration of the melt rate, perceptible in 1995 since we have a DEM at this date, has to be compared with *B*a that is measured each year: this issue will be tackled in the next section.

4.3 AL volume change: DEM subtraction versus *Ba (1962–2013)*

Firstly, regarding the only available past dataset of stake measurements on AL, we can deduce that the ablation rate, obtained by Brossard and Joly (1986) on the partial Geoffray's stake network for 1965–1975, is of the same order of magnitude (−1.05 to −0.24 m a^{-1}; Table 4) as the loss deduced by DEM differences for the 1962–1995 period (−1.09 to −0.17 m a^{-1}; Table 4). The mean annual 2008–2013 ablation rate (obtained at the position of Geoffray's stakes) is 1.8 times more negative than the mean rate calculated with the data given by Brossard and Joly (1986) for the 1965–1975 period.

Since stake values of 1965−1975 are not usable for computing an AL *B*a, (the retrieved stakes being only located in the ablation area), we used *B*a reconstructed from long time series of ML *B*a for 1968−2007 and AB *B*a for 1963−1967 in addition to the 8 years of *in-situ* measurements (2008−2015), in order to compare them to DEM differences (see the sections 2.3 and 3.5).

Results showed that for the overall period (1962−2013), the average altitude difference between DEMs (−0.441 ± 0.062 m w.e. a^{-1}) was similar to the average *B*a (−0.451 ± 0.007 m w.e. a^{-1}), indicating a good consistency between both methods to survey the glacier geometry change (Table 2). At shorter time scale, both methods also display similar rates except for the shortest period, 2009−2013 (Figure 10 and Table 2): over 1962−1995, the average *B*a (−0.422 ± 0.016 m w.e. a^{-1}) is statistically similar to DEM subtraction values (−0.384 ± 0.123 m w.e. a^{-1}) and for 1995−2013, the average *B*a (−0.505 ± 0.020 m w.e. a^{-1}) is also consistent with DEM subtraction values (−0.584 ± 0.100 m w.e. a^{-1}). As already mentioned for DEM differencing (section 4.2), the increase in the loss rate in time is more highlighted by *B*a data due to low error bars (Figure 10).

As no breakpoint was found in the whole time series of AL *B*a (computed from our stake measurements or reconstructed from ML or AB *B*a), the increase of loss rate is likely progressive through time.

All of this confirms that long term data gives accurate and similar results using *B*a and DEM at the exception of short term data that yield high error bars. The data presented in this paper reinforces the results obtained for AL by Friedt *et al.* (2012) by using a more homogenous dataset (*B*a compared to DEM difference over similar time intervals) and longer observed *B*a time series on AL. Indeed, Friedt *et al.* (2012) used a different dataset for AL: (i) a 2006 DEM that we discarded in this current investigation due to some poorly covered areas, (ii) they compared *B*a and DEMs for different years (2008−2010 for *B*a *versus* 2006−2009 for the DEMs) and (iii) over a shorter period than considered here. Similarly, on ML, Rees and Arnold (2007) also accounted for a discrepancy between 2-DEM differencing and *B*a computed from stake measurements but they could not relate the 2003-2005 LIDAR data to the *B*a of the same period as the latter were not available. Therefore, they compared the 2003−2005 DEM with mean 1977−1995 *B*a values.

4.4 AL volume change (1962−2013) with respect to catchment area

To compare the ice volume loss between different periods during which the glacier area reduced, the glacier geometry change has to be given with respect to an area common and invariant over time. We expressed the volume change in water depth (water equivalent in m) with respect to the catchment area which is considered unchanging in a glacier basin: in the case of AL, the outer edge was chosen where it crosses a stable, massive calcareous outcrop a few hundred meters upstream from the coastline (Figure 1) and which is not affected by changes in coastline position.

The AL ice loss obtained for the whole period by DEM subtraction (Table 2) was −0.215 ± 0.030 m w.e. a^{-1} with respect to the catchment area (10.577 km^2). For the same period (1962−2013), the average *B*a is −0.221 ± 0.003 m w.e. a^{-1} with respect to the catchment area, again emphasizing the consistency between the two methods.

Regarding the two periods mentioned above (1962−1995, 1995−2013), the loss rates, normalized to the catchment area, are still consistent within each period (Table 2; Figure 7 and Figure 10):

- −0.212 ± 0.008 m w.e. a^{-1} (mean *B*a for 1963–1995) *versus* −0.193 ± 0.062 m w.e. a^{-1} (mean annual 1962–1995 DEM subtraction),
- −0.222 ± 0.009 m w.e. a^{-1} (mean *B*a for 1996–2013) *versus* −0.256 ± 0.044 m w.e. a^{-1} (mean annual 1995–2013 DEM differences).

Regarding the evolution of loss rates through time, both methods confirm an increase in the loss for the second period (Figure 7). Both proxies indicate increase of the melt rate in the second time interval even if the normalization to catchment area smooths the differences between the two considered periods.

4.5 AL change with respect to glacier surface exposed to melting (1948–2013)

From 1962 to 2013, the AL regularly lost ice (–26% in volume and –23% in area). Under similar climatic conditions, we would expect that decreasing the glacier area would lead to a progressive decrease of melt rate, which is not the case for AL for which even though the area decreased, the rate of ice melt (in volume) increased. It is well-known that the relationship between glacier size and change in ice volume is not straightforward, since a glacier response time must be considered: immediate for volume and delayed for length and area (Cuffey and Paterson, 2010).

To discuss the apparent discrepancy between the overall area change and volume change, we may assess the glacier surface exposed to melting for 1948–2013 using AT data. For this purpose, we chose to compute the area of glacier surface exposed to melting by considering an average elevation of the 0°C isotherm based on the mean air temperature of summer months (MSAT), i.e. from May 1 to September 30. This particular time interval was selected as it covers most of the melting period. However, the choice of a constant period allows for the computing of an average 0°C isotherm elevation for each date, which has to be considered as relative values rather than absolute values.

For the estimate of the 0°C isotherm position, two climatic stations were used: Ny-Ålesund station (1969–2013) and Longyearbyen (1948–1968). As no longitudinal gradient of AT exists between the lower part of the AL catchment and Ny-Ålesund station, the Ny-Ålesund MSAT time series corrected for altitude−AT gradient of −0.005°C m^{-1} was directly used to estimate yearly the elevation of the 0°C isotherm over the glacier from 1969 to 2013. To extend the time period before 1969, the Longyearbyen MSAT series was used since (i) this station started earlier than that of Ny-Ålesund and (ii) both monthly AT series (limited to May to September) are very well correlated. We established the relationship at T(Ny-Ålesund) = 0.82 x T(Longyearbyen) − 0.13 where T is the MSAT in °C (r = 0.95 and n = 175 months). These MSAT values was translated into values at AL and corrected for an altitude-AT gradient, then the yearly average elevation of the 0°C isotherm for May-September over AL was assessed for 1948−2013. Then, for 7 dates for which the AL front position data are available, the area below the 0°C isotherm elevation, i.e. the area with average positive MSAT, was deduced to define a so-called “glacier area exposed to melting” and reported on Figure 11.

From 1948 to 2013, we observe an upward shift in elevation of the 0°C isotherm, regularly from 1948 (209 m a.s.l.) to 2013 (454 m a.s.l.), except for 1962−1977 (0°C isotherm slightly decreased from 276 to 267 m a.s.l.). At the same time, the glacier area decreased (Figure 11). The AL area exposed to melting substantially increased from 1.9 km^2 in 1948 to 3.5 km^2 in 2013, i.e. respectively 30% and 78% of the whole area. In 65 years, the glacier area exposed to melting was multiplied by 1.8 while the total AL area reduced by almost a third (29%). This could be the main explanation of the fact that the change of AL volume increased while its area change decreased.

The evolution of AL areas, over and under the 0°C isotherm elevation, through time is shown in Figure 12. The total glacier area reduced while the area over the 0°C isotherm elevation decreased and the area below the 0°C isotherm line displayed a noticeable decreasing trend for 1948−1995 and then a strong increase between 1995 and 2013. The breakpoint in 1995 occurs due to the increase in MSAT observed at Ny-Ålesund at this time (cf. section 3.1).

With such a change in the 0°C isotherm position towards higher elevation over the catchment, the average position of the 0°C isotherm will soon exceed the upper part of the glacier (550 m a.s.l.) during the May−September period and AAR will tend to zero at the end of the summer. Under such conditions, the glacier area will shrink and the output meltwater volume is then expected to decrease. This geometrical statement might be compensated for by climatic considerations. The melting period could extend in time, before May and/or after September, and MSAT may increase, countering once again the expected decreasing trend that should be seen in the melt rate. The whole glacier surface could be subject to only positive temperatures in the summer by ~ 2020 (see regression line of area over 0°C extended to 0 km^2 in Figure 12). Such conditions might already be met: AAR data between 2008 and 2015 often showed values at or closed to 0%, in 2011, 2013 and 2015 (Table 3)..

5. Conclusion

The changes in Austre Lovénbreen geometry were investigated using a set of data and documents whose source was heterogeneous in nature and scale (topographic map, aerial photos, satellite and airborne images). Recent annual mass balance measurements were also used based on a 36-stake network established on the Austre Lovénbreen in 2007.

1. Austre Lovénbreen, like neighbouring glaciers of the Brøgger peninsula (e.g. Midtre Lovénbreen), is shrinking. Its total retreat is 1064 ± 20 m in length (over 7 profiles) over 1948−2013, 1.82 ± 0.28 km^2 in area over the same period. The loss in volume is −129.1 ± 18.1 x 10^6 m^3 over 1962−2013. In half a century, the glacier lost almost a third of its volume, from 471 ± 74 x 10^6 in 1962 to 342 ± 46 x 10^6 m^3 in 2013.
2. Austre Lovénbreen average annual rates were the following: −16.7± 0.3 m a^{-1} in length for 1948−2013, −0.027 ± 0.002 km^2 a^{-1} in area for 1948−2013 and −2.3±0.3 x 10^6 m^3 w.e. a^{-1} for 1962−2013, i.e. −0.54 ± 0.07% a^{-1} of the 1962 glacier volume.
3. The mean annual mass balance over 1962−2013 (−0.221 ± 0.003 m

w.e. with respect to the Austre Lovénbreen catchment area) is comparable to the DEM subtraction values (−0.215 ± 0.030 m w.e. with respect to the catchment area). The good agreement between the two methods used to survey the annual glacier volume change demonstrates that the DEM difference is an efficient method if applied at dates separated by a time interval long enough for the altitude uncertainty to become negligible with respect to mass balance: in our case, such a condition is met for durations reaching a decade.

4. The perceptible breakpoint between 1990 and 1995 (decrease of area change rate from −0.032 ± 0.003 km^2 a^{-1} for 1948–1995 to −0.018 ± 0.005 km^2 a^{-1} for 1995–2013) is explained by the increased local influence of the topography of the surrounding terrain, inducing a thicker and less wide glacier terminus.
5. Regarding two periods (1962−1995, 1995−2013), the increase in the loss rate in time is more highlighted by *B*a data than DEM subtraction, due to low error bars: over 1962−1995, the average *B*a was −0.422 ± 0.016 m w.e. a^{-1} whereas it was −0.505 ± 0.020 m w.e. a^{-1} or 1995−2013). Assuming the relative volume loss remains similar to that estimated from DEM difference for 1995–2013 (–0.76 ± 0.13% a^{-1}), the glacier would have completely melted in 132 ± 27 years.
6. Between the periods used to study the glacier volume change (1962–1995 and 1995–2013), Austre Lovénbreen reduced its volume by 26% while its area dropped by 23%. AL area exposed to

> melting was modelled by assessing the 0°C isotherm elevation over the glacier by averaging May-September air temperature (from Ny-Ålesund station and extended to 1948 using the Longyearbyen air temperature) from 1948 to 2013 and applying an air temperature−altitude gradient of −0.005°C m^{-1}. The 0°C isotherm elevation rose over the glacier by 250 m on average in 65 years. The glacier area exposed to melting during the May-September period almost increased by 1.8–fold while the total Austre Lovénbreen area reduced by almost a third since 1948 (29%).

Austre Lovénbreen already experienced negative mass balance over the entire glacier surface (for instance in 2011 and 2013 when AAR was at or closed to 0%). In 2013, only 1.0 km^2 of the total glacier area (4.48 km^2) was over the 0°C isotherm. If this continues, within a few years, the glacier area exposed to melting will reduce as the entire present-day accumulation area will be under the 0°C isotherm while the snout will keep on retreating. This would then eventually imply a reduction of ice melt if air temperatures remain at least similar.

Acknowledgements

The project was funded by the French Agence Nationale pour la Recherche (ANR) (programme blanc, the projects Hydro-Sensor-FLOWS and Cryo-Sensors) and by the Institut polaire français Paul-Emile Victor (IPEV, programme 304). The authors wish to acknowledge the French-German AWIPEV Arctic collaborative base for having provided logistic support in the field. G. Rees and J. Kohler, who kindly provided useful data needed for this work, are warmly thanked for their contribution. Anonymous reviewers are thanked for critically reading the manuscript and suggesting substantial improvements.

References

Barrand, N. E., James, T. D. and Murray, T., 2010. Spatio-temporal variability in elevation changes of two high-Arctic valley glaciers. *Journal of glaciology,* 56. 771–780.

Bernard, E., 2011. *Les dynamiques spatio-temporelles d'un petit hydro-système arctique : approche nivo-glaciologique dans un contexte de changement climatique contemporain (bassin du glacier Austre Lovén, Spitsberg, 79°N).* PhD thesis, Université de Franche-Comté, Besançon, France, 400 p.

Bernard E., Friedt J.M., Saintenoy A., Tolle F., Griselin M. and Marlin C., 2014. Where does a glacier end? GPR measurements to identify the limits between valley slopes and actual glacier body. Application to the Austre Lovénbreen, Spitsbergen. *International Journal of Applied Earth Observation and Geoinformation*, 27, 100–108.

Bernard, E., Friedt, J.-M., Tolle, F., Griselin, M., Martin, G., Laffly, D., and Marlin, C., 2013. Monitoring seasonal snow dynamics using ground based high resolution photography (Austre Lovénbreen, Svalbard, 79°N). *J. of Photogrammetry and Remote Sensing*, 75, 92–100.

Bernard, E., Tolle F., Griselin, M., Laffly, D., and Marlin, C., 2009. Quantification des hauteurs de neige et des températures de l'air à la surface d'un glacier : du terrain à l'interpolation, confrontation de méthodes. *Actes des IX[es] Rencontres de ThéoQuant,* Besançon, France, 4-6 mars 2009.

Brandt, O. and Kohler, J., 2006. A long-term Arctic snow depth record from Abisko, northern Sweden, 1913–2004. *Polar Research,* 25(2), 91-113.

Bring, A. and Destouni, G., 2013. Hydro-climatic changes and their monitoring in the Arctic: Observation-model comparisons and prioritization options for monitoring development. *J. of Hydrology*, 492, 273–280.

Brossard, Th. and Joly, D., 1986. Le complexe géomorphologique aval des glaciers Lovén Est et Central (Svalbard). *Cahiers de Géographie de Besançon (Nlle série)*, 2, 5–58.

Cogley, J.G., R. Hock, L.A. Rasmussen, A.A. Arendt, A. Bauder, R.J. Braithwaite, P. Jansson, G. Kaser, M. Möller, L. Nicholson and M. Zemp, 2011. Glossary of Glacier Mass Balance and Related Terms, *IHP-VII Technical Documents in Hydrology,* 86, IACS Contribution No. 2, UNESCO-IHP, Paris.

Corbel J., 1966. Spitsberg 1964 et premières observations 1965. CNRS-RCP 42, éd. Audin, 350 p.

Corbel J., 1970. Le Spitsberg. Présentation géographique – mission française 1966. *Mémoire et documents*, Centre Documentation cartographique et géographique du CNRS, 10, 23-35.

Cufffey, K. and Paterson, W. 2010. The Physics of Glaciers. Elsevier, Burlington, MA, USA. ISBN 978-0-12-369461-4, 704p.

Dyurgerov, M., Bring, A. and Destouni, G., 2010. Integrated assessment of changes in freshwater inflow to the Arctic Ocean. *J. Geophys. Res.,* 115

(D12). doi:10.1029/2009JD013060.

Dyurgerov, M., Meier, M. F., and Bahr, D. B., 2009. A new index of glacier area change; a tool for glacier monitoring, *Journal of Glaciology*, 55(192): 710–716.

eKlima, 2013. See the database on the web portal which gives free access to the climate database of the Norwegian Meteorological Institute. http://eklima.met.no.

Fontain A.G. and Vecchia A., 1999. How many stakes are required to measure the mass balance of a glacier? *Geograkiska Annaler*, 81 A (4): 563–573.

Førland, E.J., Benestad, R., Hanssen-Bauer, I., Haugen, J.E. and Skaugen T.E., 2011. Temperature and Precipitation Development at Svalbard 1900–2100. *Advances in Meteorology*, ID 893790. doi:10.1155/2011/893790.

Friedt, J. M., Tolle, F., Bernard, E., Griselin, M., Laffly, D. and Marlin, C., 2012. Assessing the relevance of digital elevation models to evaluate glacier mass balance: application to Austre Lovénbreen (Spitsbergen, 79°N). *Polar Record,* 48, 2–10.

Geoffray, H., 1968. *Étude du bilan hydrologique et de l'érosion sur un bassin partiellement englacé : Spitsberg, baie du Roi, 79°N.* PhD thesis, Université de Brest, Brest, France, 103 p.

Gregory, J.M., White, N.J., Church, J.A., Bierkens, M.F.P., Box, J.E. van den Broeke, M.R., Cogley, . J.G., Fettweis, X., Hanna, E. Huybrechts, P., Konikow, L.F., Leclercq, P.W., Marzeion, B., Oerlemans, J., Tamisiea, M.E., Wada, Y., Wake L.M. and van de Wal, R.S.W, 2013. Twentieth-Century Global-Mean Sea Level Rise: Is the Whole Greater than the Sum of the Parts?, *Journal of Climate*, 26, 4476–4499.

Griselin, M., 1982. *Les écoulements solides et liquides sur les marges polaires, exemple du bassin de Lovén Est, 79°N, Spitsberg.* PhD thesis. Université de Nancy-2, Nancy, France, 500 p.

Griselin, M., 1985. L'abondance annuelle et le bilan hydrologique d'un bassin partiellement englacé de la côte nord-ouest du Spitsberg, *Norois,* 32(125), 19–33.

Griselin, M. and Marlin, C., 1999. Approche quantitative et géochimique du gradient altitudinal des précipitations sur un bassin versant partiellement englacé de la côte occidentale du Spitsberg. *La Houille Blanche*, 5, 125–136.

Haakensen, N., 1986. Glacier mapping to confirm results from mass-balance measurements. *Annals of Glaciology*, 8, 73–75.

Hagen, J.O. and Liestøl, O., 1990. Long-term glacier mass-balance investigations in Svalbard. *Annals of Glaciology,* 14, 102–106.

Hagen, J.O., Liestøl, O., Roland, E. and Jorgensen, T., 1993. *Glacier atlas of Svalbard and Jan Mayen.* Norsk Polarintitutt Meddelelser, 129, 160 p.

Hagen, J.O., Melvold, K., Pinglot, F. and Dowdeswel, J. A., 2003. On the net mass balance of the glaciers and ice caps in Svalbard, Norwegian Arctic. *Arctic, Antarctic, and Alpine Research,* 35(2), 264–270.

Hansen, S., 1999. *A photogrammetry, climate-statistical and geomorphological approach to the post Little Ice Age changes of the Midtre Lovénbreen glacier, Svalbard,* Master thesis, University of Tromsø and University of Copenhagen, 92 p.

Hock, R., 2005. Glacier melt: a review of processes and their modelling.

Progress in Physical Geography, 29(3), 362–391.

James, T. D., Murray, T., Barrand, N. E., Sykes, H. J., Fox, A. J., and King, M. A., 2012. Observations of enhanced thinning in the upper reaches of Svalbard glaciers, *The Cryosphere*, 6, 1369–1381.

Joly D. 1994. *Ambiances climatiques instantanées au Spitsberg; pour une approche méthodique par niveau d'échelle.* Annales Littéraires de l'Université de Franche-Comté, n°529, Diffusion Les Belles Lettres, Paris.

Kohler, J., James, T.D., Murray, T., Nuth, C., Brandt, O., Barrand, N.E., Aas, H.F. and Luckman, A., 2007. Accelerating in thinning rate on western Svalbard glaciers. *Geophysical Research Letters,* 24 (L18502). doi: 1029/2007GL030681.

Kohler, J., Nordli, Ø., Brandt, O., Isaksson, E., Pohjola, V., Martma, T., and Aas, H.F., 2003. *Svalbard temperature and precipitation, late 19th century to the present.* Final report on ACIA-funded project. 21 p.

Korona, J., Berthier, E., Bernard, M., Remy, F., and Thouvenot, E., 2009. SPIRIT. SPOT 5 stereoscopic survey of Polar Ice: Reference Images and Topographies during the fourth International Polar Year (2007-2009). *Journal of Photogrammetry and Remote Sensing,* 64, 204–212.

Lefauconnier, B. and Hagen, J.O., 1990. Glaciers and climate in Svalbard, statistical analysis and reconstruction of the Brøgger glacier mass balance for the last 77 years. *Annals of Glaciology,* 14, 148-152.

Lefauconnier, B., Hagen, J-O, Ørbæk, J.B., Melvold, K. and Isaksson E., 1999. Glacier balance trends in the Kongsfjord area, western Spitsbergen, Svalbard, in relation to the climate. *Polar Research,* 18(2), 307–313.

Liestøl, O. 1993. Glacier of Svalbard, Norway. US Geological Survey

Professional paper 1386–E–5.

Meier, M.F., M.B. Dyurgerov, U.K. Rick, S. O'Neel, W.T. Pfeffer, R.S. Anderson, S.P. Anderson, and A.F. Glazovsky. 2007. Glaciers dominate eustatic sea-level rise in the 21st century. *Science* 317, 1064-1067

Mingxing, X., Ming, Y., Jiawen, R., Songtao, A., Jiancheng, K., Dongchen, E., 2010. Surface mass balance and ice flow of the glaciers Austre Lovénbreen and Pedersenbreen, Svalbard, Arctic, *Chinese Journal of Polar Science*. 21 (2), 147–159.

Moholdt, G., Nuth, C., Hagen, J.O. and Kohler, J., 2010. Recent elevation changes of Svalbard glaciers derived from ICESat laser altimetry. *Remote Sensing of Environment,* 114 (11), 2756–2767.

Murray, T., Booth, A. and Rippin, D., 2007. Limitations of glacier ice-water content estimated using velocity analysis of surface ground-penetrating radar surveys, *Journal of Environmental and Engineering Geophysics,* 12, 87–99.

Oosterbaan, R.J., 1994. Frequency and regression analysis of hydrologic data. Chapter 6 in: H.P. Ritzema (Ed.), *Drainage Principles and Applications,* Publication 16, second revised edition, 1994, International Institute for Land Reclamation and Improvement (ILRI), Wageningen, The Netherlands.

Østrem, G. and Brugman, M., 1991. *Glacier mass-balance measurements: a manual for field and office work,* National Hydrology Research Institute – NHRI Science report, No. 4, 220 p.

Paterson, W. S. B., 1994. The Physics of Glaciers (Third edition), Pergamon, Oxford, 480 p.

Pillewizer, W., 1967. Zur Karte des Kongsvegen-Kronebre 1/50,000, Estspitzbergen. Petermanns Geographische Mitleilungen, Jahrg. Ill, *Quartalsht.* 2, 153–157.

Radić, V., Bliss, A., Beedlow, A. C., Hock, R., Miles, E. and Cogley, J. G. (2013). Regional and global projections of twenty-first century glacier mass changes in response to climate scenarios from global climate models. *Climate Dynamics*, 42(1-2), 37-58.

Rees, W.G. and Arnold, N.S., 2007. Mass balance and dynamics of a valley glacier measured by high-resolution LiDAR. *Polar Record, 43,* 311-319.

Rignot, E., and P Kanagaratnam, P., 2006. Changes in the velocity structure of the Greenland Ice Sheet, *Science*, 311 (5763), 986-990

Rippin, D., Willis, I., Arnold, N., Hodson, A., Moore, J., Kohler, J. and Bjornsson, H., 2003. Changes in geometry and subglacial drainage of Midre Lovénbreen, Svalbard, determined from digital elevation models, *Earth Surface Processes and Landforms,* 28, 273–298.

Saintenoy, A., Friedt, J.-M., Booth, A.D., Tolle, F., Bernard, E., Laffly D., Marlin, C. and Griselin M., 2013. Deriving ice thickness, glacier volume and bedrock morphology of Austre Lovénbreen (Svalbard) using GPR. *Near Surface Geophysics*, 11, 253–261.

Stocker, T.F., D. Qin, G.-K. Plattner, M. Tignor, S.K. Allen, J. Boschung, A. Nauels, Y. Xia, V. Bex and P.M. Midgley, 2013. IPCC: Climate Change 2013: The Physical Science Basis. Contribution of Working Group I to the Fifth Assessment Report of the Intergovernmental Panel on Climate Change. Eds. Cambridge University Press, Cambridge, United Kingdom and New York, NY, USA, 1535 pp.

doi:10.1017/CBO978110741532

Vincent, M. and Geoffray, H., 1970. Etude d’un régime glaciaire en fonction de la température et de l’ensoleillement, Baie du Roi, (été 1966), *Mémoires et documents du CNRS,* 10, 219–229.

Vincent, C., Vallon, M., Reynaud, L. and Le Meur, E., 2000. Dynamic behaviour analysis of glacier de St Sorlin, France from 40 years of observations, 1957-1997. *Journal of glaciology,* 46, 499–506.

Vivian, H., 1964. Premières observations sur le régime estival des torrents glaciaires du Spitsberg (79° latitude Nord), *Norois,* 43, 283–307.

WGMS, 2016. World glacier monitoring service under the hospice of ICSU, IUGG, UNEP, UNESCO, WMO. http://www.wgms.ch.

	AL retreat (central axis)			AL retreat (7 fanned out profiles)			Glacier area	Length of glacier boundary	
Year	Length between 2 dates (m)	Cumulative length from 1948 (m)	Mean annual rate (m a^{-1})	Length between 2 dates m	Cumulative length from 1948 (m)	Mean annual rate (m a^{-1})	Mean area (km^2)	**Glacier** perimeter[a] (km)	Length of glacier front (km)
1948		0			0		6.30±0.17	16.87	4.58
1962	209±20	209±20	14.9±1.4	206±20	206±20	14.7±1.4	5.85±0.16	16.21	3.91
1966	140±20	349±20	35.0±5.0	81±20	287±20	20.3±5.0	5.65±0.16	16.25	3.96
1971	86±20	435±20	17.2±4.0	85±20	372±20	17.0±4.0	5.49±0.16	16.01	3.72
1977	93±20	528±20	15.5±3.3	91±20	463±20	15.2±3.3	5.31±0.16	15.71	3.42
1990	283±20	811±20	21.8±1.5	240±20	703±20	18.5±1.5	4.92±0.15	14.96	2.67
1995	30±20	841±20	6.0±4.0	86±20	789±20	17.2±4.0	4.80±0.15	14.85	2.56
2005	185±20	1026±20	18.5±2.0	143±20	932±20	14.3±2.0	4.61±0.14	14.39	2.09
2008	100±20	1126±20	33.3±6.7	61±10	993±20	20.3±6.7	4.56±0.14	14.32	2.02
2009	30±10	1156±20	30.0±10.0	13±10	1006±20	13.0±10.0	4.54±0.14	14.40	2.11
2010	12±10	1168±20	12.0±10.0	10±10	1016±20	10.0±10.0	4.53±0.14	14.22	1.93
2011	49±10	1217±20	49.0±10.0	27±10	1043±20	27.0±10.0	4.51±0.14	14.23	1.94
2012	19±10	1236±20	19.0±10.0	12±10	1055±20	12.0±10.0	4.50±0.14	14.18	1.89
2013	11±10	1247±20	11.0±10.0	9±10	1064±20	9.0±10.0	4.48±0.14	14.04	1.75
Mean value			19.2±0.3			16.7±0.3	5.39±0.15	15.05 (SD=0.96)	2.75 (SD=0.96)

[a]The glacier perimeter is calculated by summing the length of glacier front (variable in time; see the thin lines for the different years on figure 3) to that of the upper part of the glacier (considered constant at 12.29 km; see the yellow, thick solid line on figure 3).

Table 1: Austre Lovénbreen (AL) retreat in length and in area, glacier perimeter and length of glacier front from 1948 to 2013.

Period	Change in glacier area	DEM subtraction: Net loss in ice			DEM subtraction: Net loss in water equivalent[a]				Annual mass balance: Water equivalent[a]	
	(km^2 a^{-1})	(10^6 m^3)	(10^6 m^3 a^{-1})	(m a^{-1})[b]	(x10^6 m^3)	(x10^6 m^3 a^{-1})	(m a^{-1})[b]	(m a^{-1})[c]	(m a^{-1})[b]	(m a^{-1})[c]
1962[d]-1995 33 years (5.32 km^2)	−0.032 ±0.003	−74.9 ±23.9	−2.3 ±0.7	−0.427 ±0.136	−67.4 ±21.5	−2.0 ±0.7	−0.384 ±0.123	−0.193 ±0.062	−0.422 ±0.016	−0.212 ±0.008
1995[e]-2009 14 years (4.67 km^2)	−0.018 ±0.007	−47.1 ±9.3	−3.4 ±0.7	−0.720 ±0.143	−42.4 ±8.4	−3.0 ±0.6	−0.648 ±0.129	−0.286 ±0.057	−0.466 ±0.026	−0.206 ±0.011
2009[f]-2013 4 years (4.51 km^2)	−0.015 ±0.020	−7.1 ±4.5	−1.8 ±1.1	−0.394 ±0.250	−6.4 ±4.1	−1.6 ±1.0	−0.354 ±0.225	−0.151 ±0.096	−0.643 ±0.045	−0.274 ±0.019
1995[e]-2013 18 years (4.64 km^2)	−0.018 ±0.005	−54.2 ±9.3	−3.0 ±0.5	−0.649 ±0.111	−48.8 ±8.4	−2.7 ±0.5	−0.584 ±0.100	−0.256 ±0.044	−0.505 ±0.020	−0.222 ±0.009
1962[d]-2013 51 years (5.17 km^2)	−0.026 ±0.002	−129.1 ±18.1	−2.5 ±0.4	−0.490 ±0.069	−116.2 ±16.3	−2.3 ±0.3	−0.441 ±0.062	−0.215 ±0.030	−0.451 ±0.007	−0.221 ±0.003

[a] Volume of water = volume of ice x ice density (0.9).

[b] Calculated in relation to a mean area of the glacier.

[c] Calculated in relation to the Austre Lovénbreen catchment area (10.577 km^2).

[d] 1963 for *B*a.

[e] 1996 for *B*a.

[f] 2010 for *B*a.

Table 2: Calculated Austre Lovénbreen area and volume changes for five periods: 1962–1995, 1995–2009, 2009–2013, 1995–2013 and 1962–2013.

Year	Annual mass balance, *B*a (m): Ice in relation to glacier area [a]	Annual mass balance, *B*a (m): Water equivalent in relation to glacier area [a]	Annual mass balance, *B*a (m): Water equivalent in relation to catchment area [b]	Accumulation Area Ratio (AAR)
2008	−0.115	−0.104	−0.045	0.66
2009	−0.164	−0.148	−0.063	0.33
2010	−0.183	−0.165	−0.071	0.45
2011	−1.170	−1.053	−0.451	0.00
2012	−0.267	−0.241	−0.103	0.39
2013	−1.233	−1.111	−0.475	0.00
2014	+0.011	+0.010	+0.004	0.62
2015	−0.613	−0.552	−0.236	0.05
Mean				
2010−2013	−0.713	−0.643	−0.274	0.21
2008−2015	−0.468	−0.421	−0.180	0.31

[a] glacier area of 4.53 km^2 (mean 2008−2013)

[b] 10.577 km^2

Table 3: Austre Lovénbreen annual mass balances and accumulation area ratio for 2008–2015. The uncertainty on *B*a is ±0.10 m in ice, ±0.09 m in water equivalent and ±0.04 m in water equivalent with respect to catchment area.

	Net mass balance			DEM subtraction			
	(m)	(m a^{-1})		(m)		(m a^{-1})	
Stake ID[a]	1965–1975[b]	1965–1975[b]	2008–2013[c]	1995–1962[c]	2013–1995[c]	1995–1962[c]	2013–1995[c]
1	−10.5	−1.05	−2.47	−36	−34	−1.09	−1.90
2	−7.75	−0.78	−1.65	−20	−18	−0.59	−1.02
3	−5.55	−0.56	−0.95	−12	−12	−0.35	−0.69
4	−4.95	−0.50	−0.70	−9	−10	−0.29	−0.55
5	−4.75	−0.48	−0.81	−11	−12	−0.34	−0.65
6	−4.70	−0.47	−0.60	−6	−10	−0.17	−0.55
7	−2.35	−0.24	−0.57	−12	−8	−0.35	−0.43
Mean	−5.79	−0.58	−1.11	−15.1	−14.9	−0.45	-0.83

[a] Location in Figure 2

[b] After Geoffray's stake network (1968) and Brossard and Joly (1986)

[c] This study.

Table 4: Net mass balance (1965–1975 and 2008–2013) and DEM subtraction (1995–1962 and 2013–1995) of Austre Lovénbreen at the locations of the seven stakes of Geoffray (1968).

Figure captions

Figure 1: Location of Austre Lovénbreen within the Svalbard archipelago and the Brøgger Peninsula. AL : Austre Lovénbreen; ML : Midtre Lovénbreen; AB: Austre Brøggerbreen. On the Figure 1c, the dashed line indicates the position of a calcareous, massive outcrop. The blue dot is the outlet considered for delineating the watershed boundaries of AL

Figure 2: Documents and stake networks used to survey the Austre Lovénbreen geometry change. In the Figures 2d and 2e, the pink line is the upper AL watershed boundary, the green line is the downstream watershed boundary (i.e. the proglacial moraine limit upstream the outlet) and the blue line is the 2009 glacier limit.

Figure 3: Front position of Austre Lovénbreen between 1948 and 2013. Outside the front area, since the change of the glacier limits were considered negligible, we used the limits visible on a Formosat-2 image of August 2009.

Figure 4: Mean annual air temperature (MAAT) and mean summer air temperature (MSAT) in Ny-Ålesund for 1970–2013. The data are given in hydrological years, i.e. from October 1 to September 30. Summer is considered from May 1 to September 30.

Figure 5: Austre Lovénbreen length and area changes over 1948-2013.

a. The length reduction *versus* time. The dashed line is derived best-fit line of the average of 7 profiles (slope of –16.4 m a^{-1}) and the solid line is for the mean central flowline (slope of −19.3 m a^{-1}).

b. The area reduction *versus* time. The black, dashed is the derived best-fit line of all datapoints (−0.027 km^2 a^{-1} for 1948–2013) segmented into two lines by a breakpoint between 1990 and 1995 (−0.032 km^2 a^{-1} for 1948–1995 and –0.018 km^2 a^{-1} for 1995–2013).

Figure 6: Maps of DEM differences of Austre Lovénbreen for four periods: 1962−1995, 1995−2009, 2009−2013 and 1962−2013. For 2009−2013, the colour scale is different than that of the 3 other maps since the change of altitude for four years is very low.

Figure 7: Time-series of AL annual mass-balances from AL measurements (dark blue) and reconstituted from mass balances from the ML (solid light blue line) and from AB (dashed light blue line). The average values of both AL *B*a and DEM subtraction are also indicated with error bars (grey rectangles).

Figure 8: Correlation between annual mass balances between AL and 2 glaciers of the

Brøgger peninsula: Austre Lovénbreen (AL) *versus* Midtre Lovénbreen (ML) for 2008–2015 (a) and ML *versus* Austre Brøggerbreen (AB) for 1968-1988.

Figure 9: Cross-sections of the glacier along the central flowline (Austre Lovénbreen) in 1962, 1995, 2009 and 2013. The upper insert gives the ice thickness at a distance of 500 m from the AL front of 1962, 1995, 2009 and 2013 respectively.

Figure 10: Comparison of methods for estimating AL volume change (*B*a and DEM subtraction) for four periods (1962–2013, 1962–1995, 1995–2013 and 2009–2013).

Figure 11: Elevation of the average 0°C-isotherm over AL for 7 years (1948, 1962, 1977, 1995, 2005, 2009 and 2013). The position of the 0°C isotherm elevation was estimated from the Ny-Ålesund temperature data of summer months (May-September) corrected from an elevation gradient of –0.005°C m^{-1}. The values in km^2 refer to the glacier area under (light blue) or over (dark blue) the 0°C-isotherm. The values in m are the elevation of the 0°C isotherm. Glacier elevation for 1948 and 1977 is that of 1962 and for 2005 it is that of 2009.

Figure 12: Areas (total, over and under 0°C isotherm) as a function of time (1948–2013).

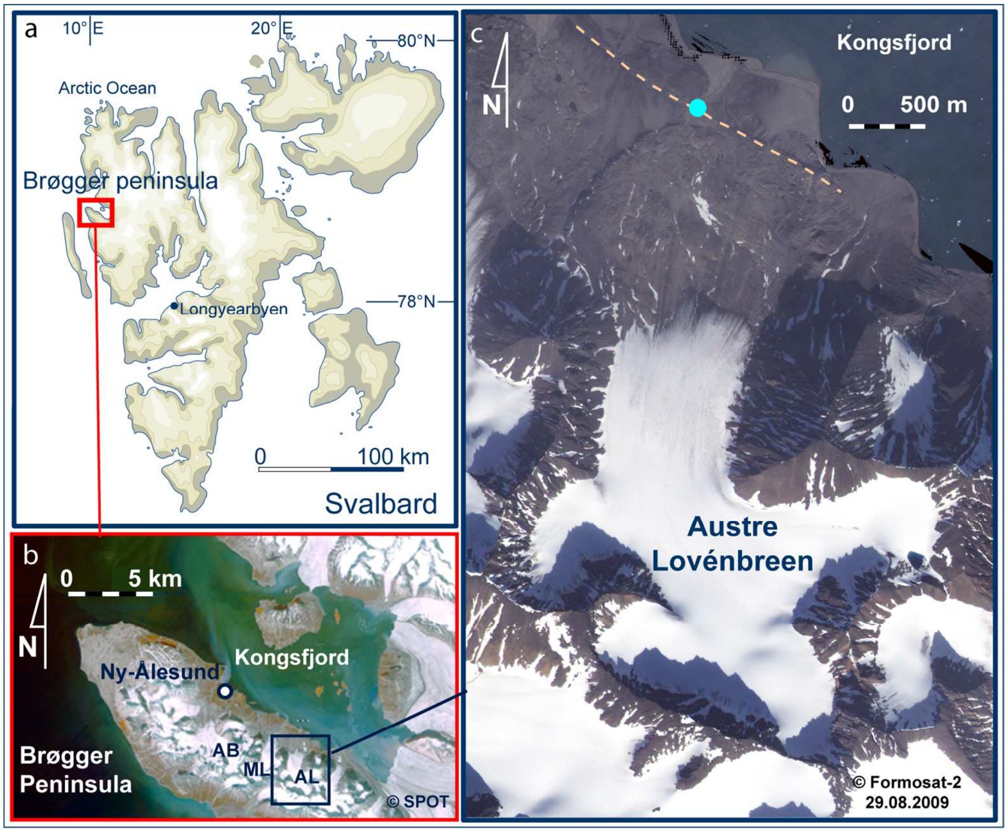

Figure 1: Location of Austre Lovénbreen within the Svalbard archipelago and the Brøgger Peninsula. AL : Austre Lovénbreen; ML : Midtre Lovénbreen; AB: Austre Brøggerbreen. On the Figure 1c, the dashed line indicates the position of a calcareous, massive outcrop. The blue dot is the outlet considered for delineating the watershed boundaries of AL

147x121mm (300 x 300 DPI)

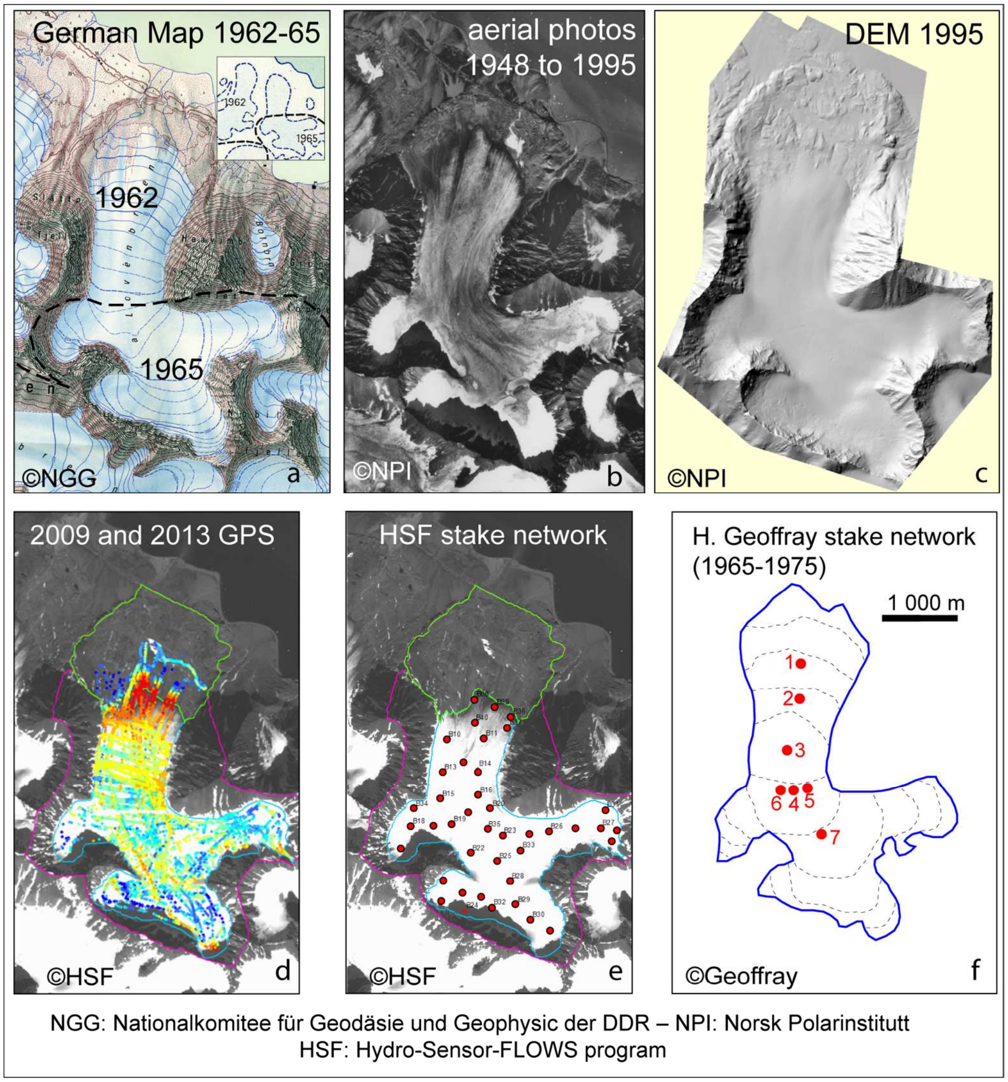

Figure 2: Documents and stake networks used to survey the Austre Lovénbreen geometry change. In the Figures 2d and 2e, the pink line is the upper AL watershed boundary, the green line is the downstream watershed boundary (i.e. the proglacial moraine limit upstream the outlet) and the blue line is the 2009 glacier limit.

143x154mm (300 x 300 DPI)

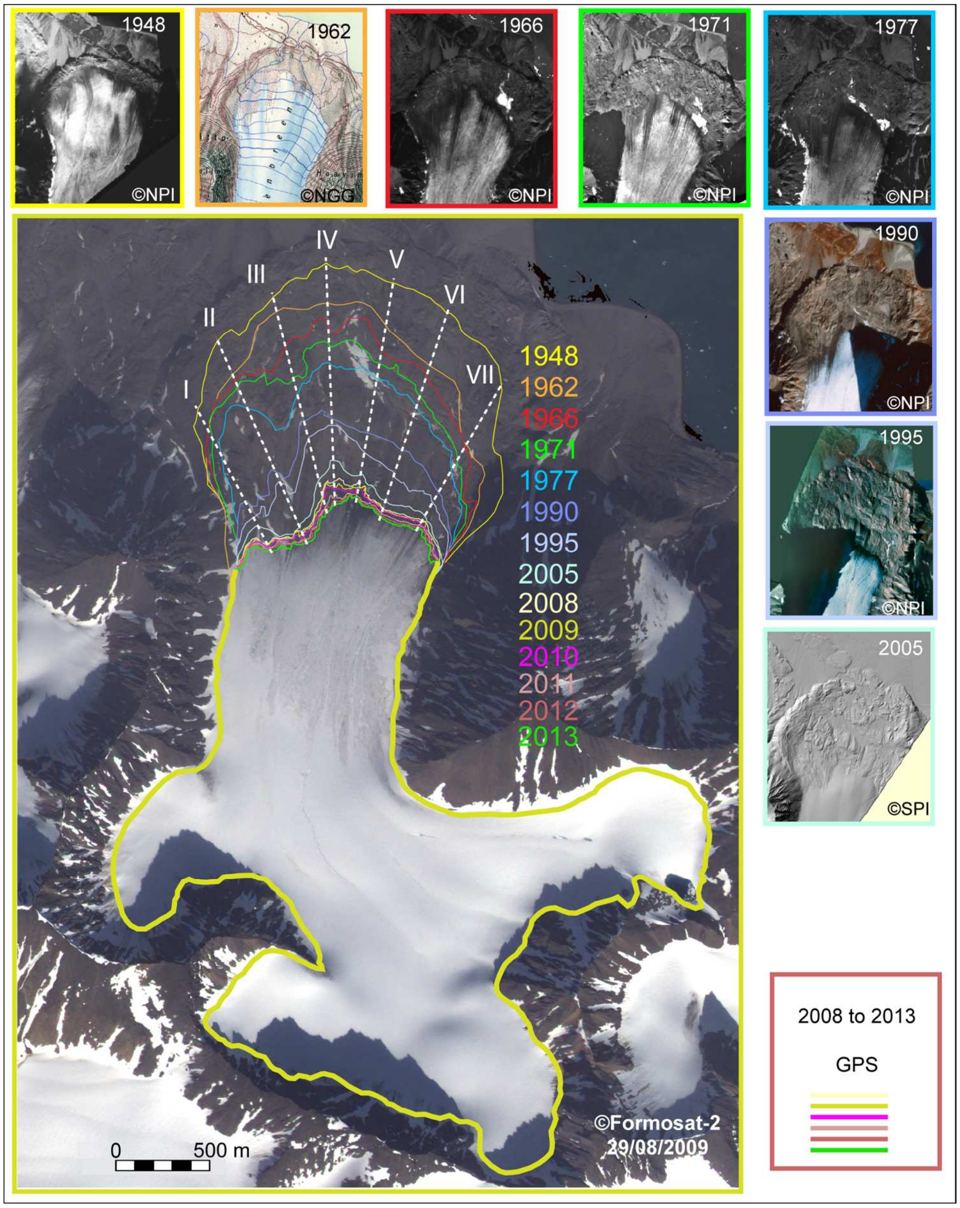

Figure 3: Front position of Austre Lovénbreen between 1948 and 2013. Outside the front area, since the change of the glacier limits were considered negligible, we used the limits visible on a Formosat-2 image of August 2009.

148x186mm (300 x 300 DPI)

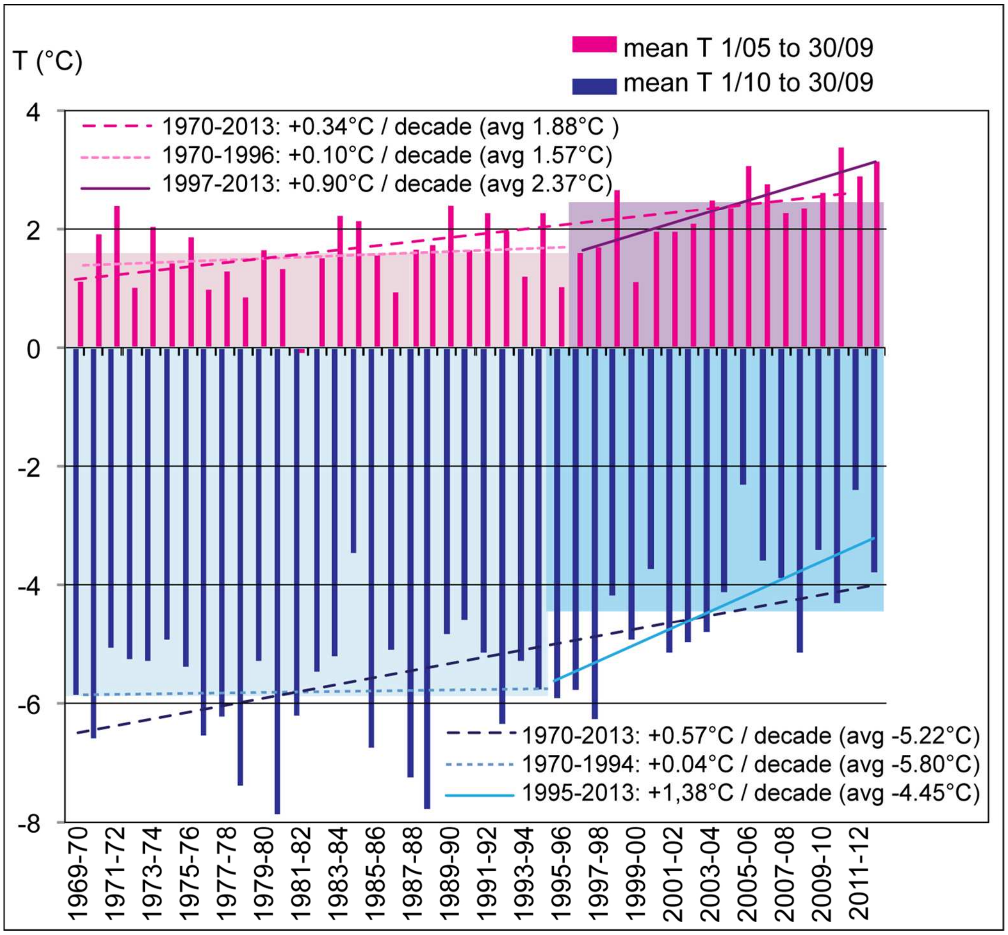

Figure 4: Mean annual air temperature (MAAT) and mean summer air temperature (MSAT) in Ny-Ålesund for 1970–2013. The data are given in hydrological years, i.e. from October 1 to September 30. Summer is considered from May 1 to September 30.

133x124mm (300 x 300 DPI)

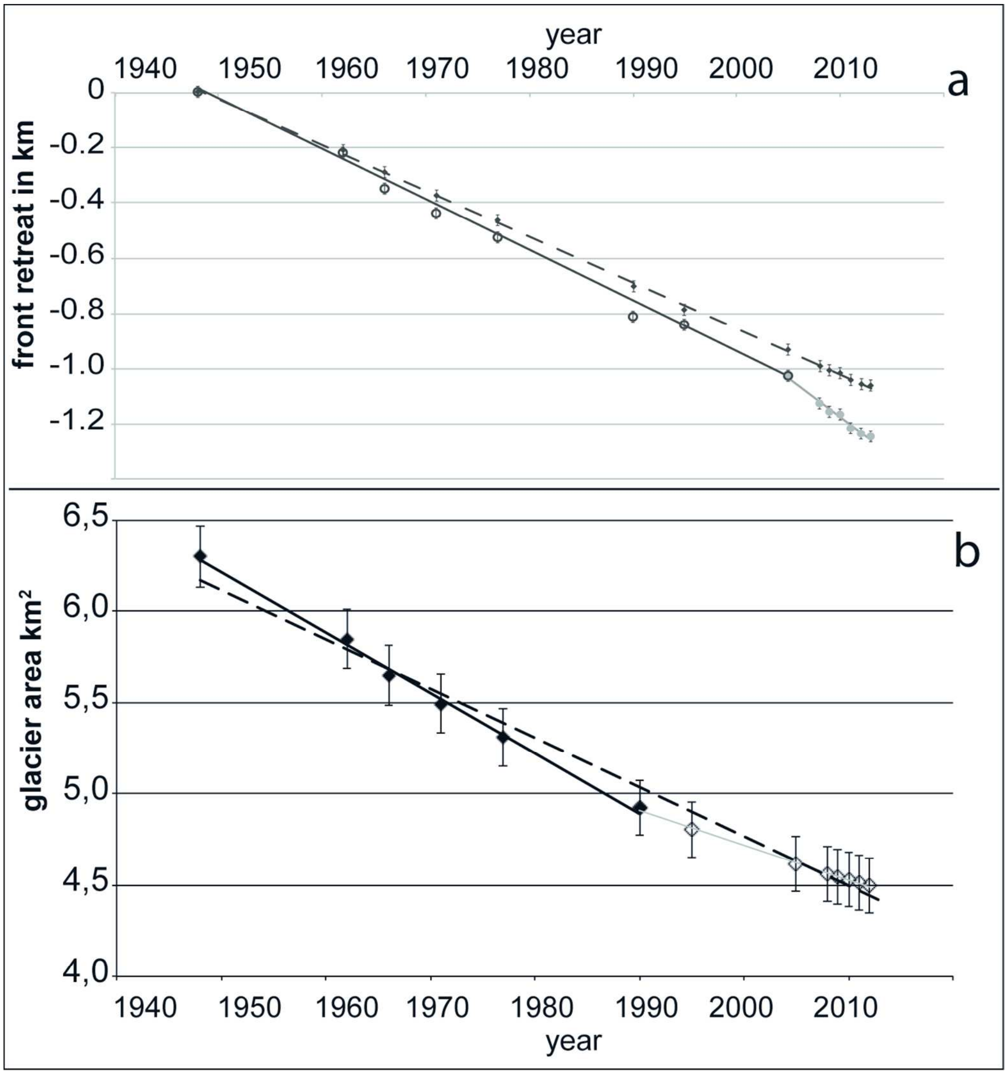

Figure 5: Austre Lovénbreen length and area changes over 1948-2013.
a. The length reduction *versus* time. The dashed line is derived best-fit line of the average of 7 profiles (slope of −16.4 m a^{-1}) and the solid line is for the mean central flowline (slope of −19.3 m a^{-1}).
b. The area reduction versus time. The black, dashed is the derived best-fit line of all datapoints (−0.027 km^2 a^{-1} for 1948–2013) segmented into two lines by a breakpoint between 1990 and 1995 (−0.032 km^2 a^{-1} for 1948–1995 and −0.018 km^2 a^{-1} for 1995–2013).

119x127mm (300 x 300 DPI)

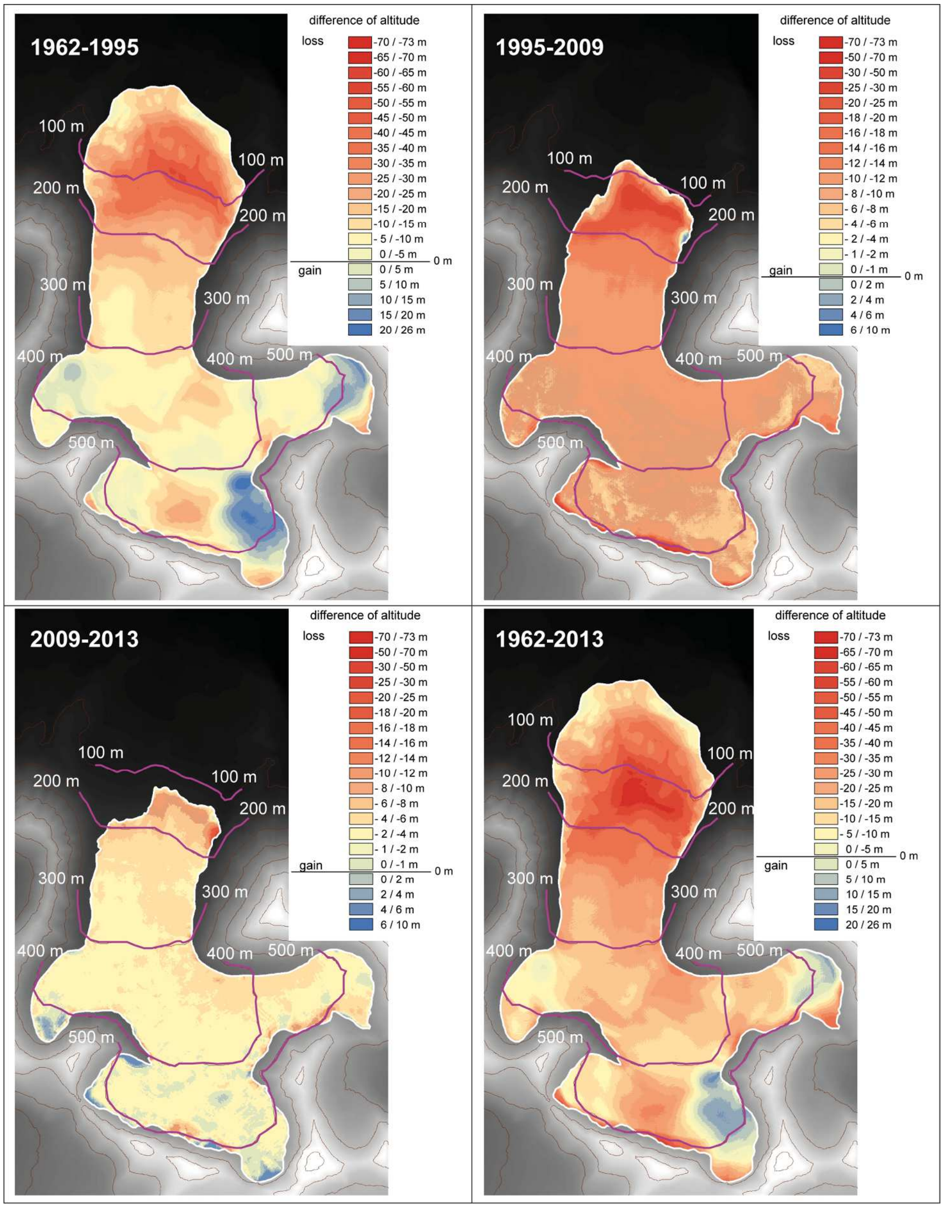

Figure 6: Maps of DEM differences of Austre Lovénbreen for four periods: 1962-1995, 1995-2009, 2009-2013 and 1962-2013. For 2009-2013, the colour scale is different than that of the 3 other maps since the change of altitude for four years is very low.

174x222mm (300 x 300 DPI)

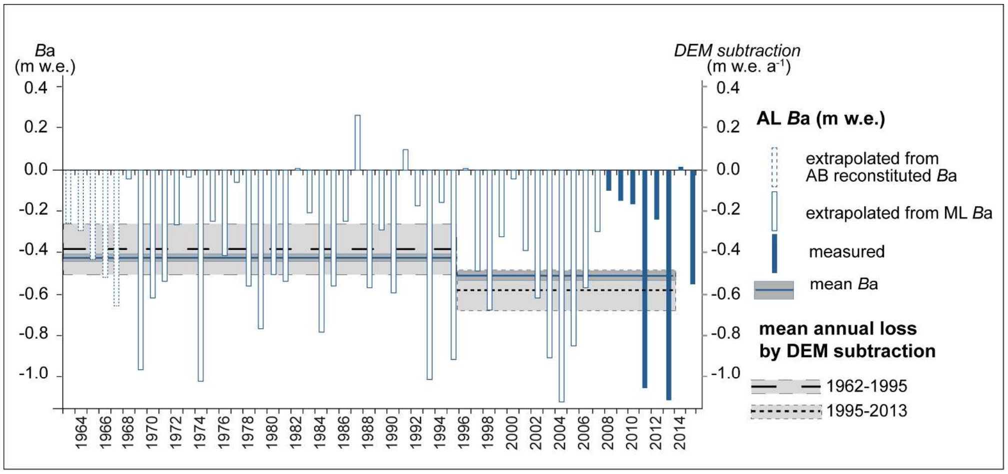

Figure 7: Time-series of AL annual mass-balances from AL measurements (dark blue) and reconstituted from mass balances from the ML (solid light blue line) and from AB (dashed light blue line). The average values of both AL *B*a and DEM subtraction are also indicated with error bars (grey rectangles).

205x96mm (300 x 300 DPI)

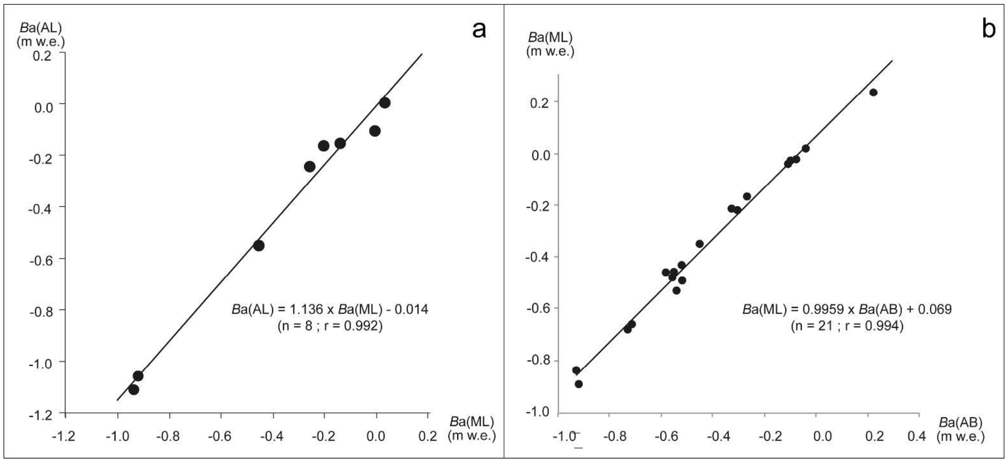

Figure 8: Correlation between annual mass balances between AL and 2 glaciers of the Brøgger peninsula: Austre Lovénbreen (AL) versus Midtre Lovénbreen (ML) for 2008-2015 (a) and ML versus Austre Brøggerbreen (AB) for 1968-1988.

259x117mm (300 x 300 DPI)

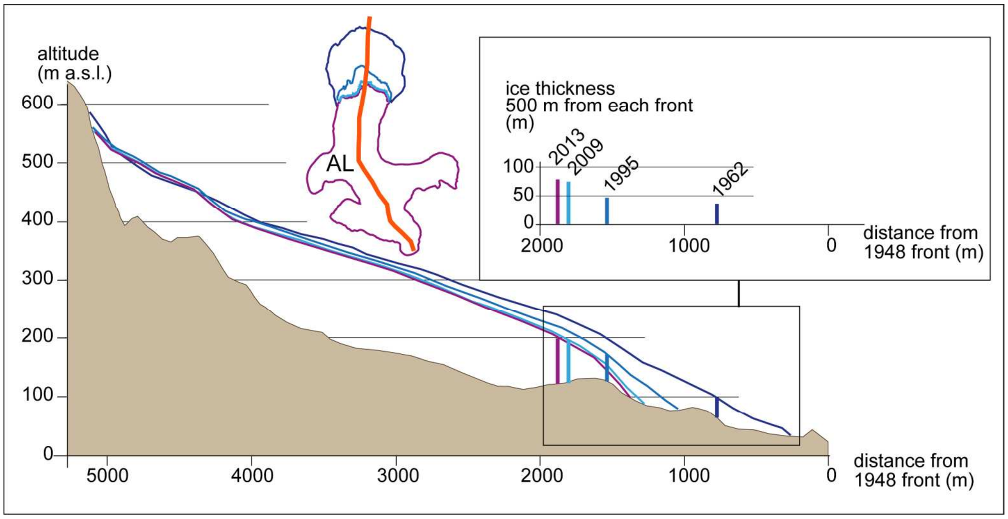

Figure 9: Cross-sections of the glacier along the central flowline (Austre Lovénbreen) in 1962, 1995, 2009 and 2013. The upper insert gives the ice thickness at a distance of 500 m from the AL front of 1962, 1995, 2009 and 2013 respectively.

183x94mm (300 x 300 DPI)

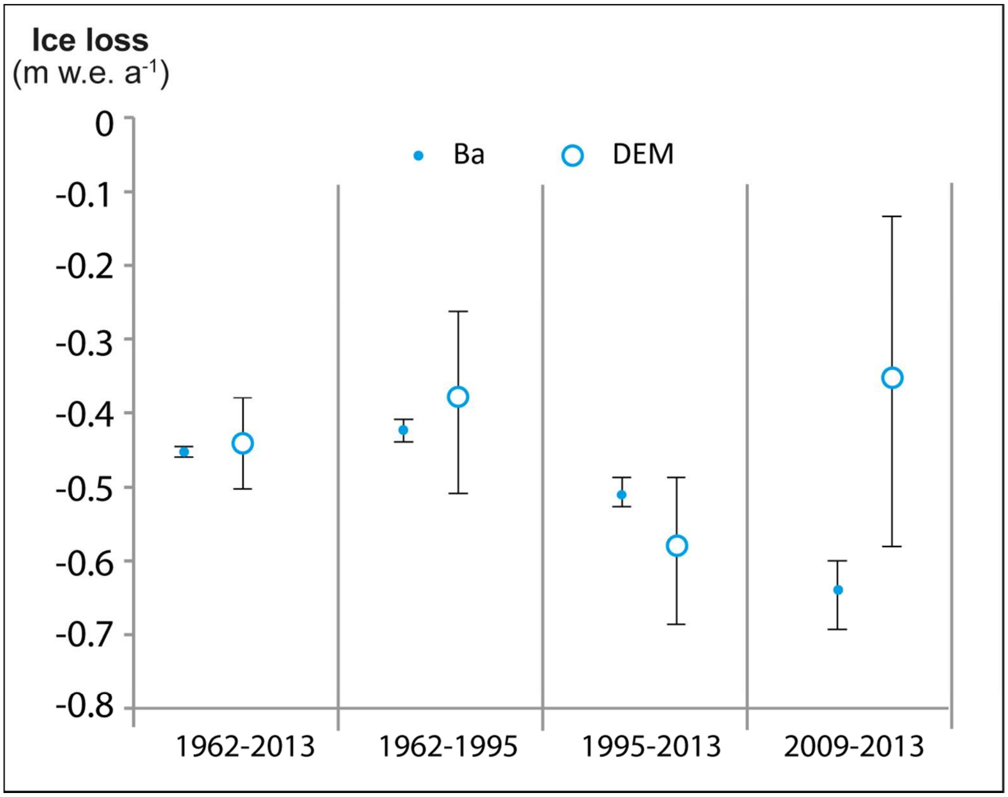

Figure 10: Comparison of methods for estimating AL volume change (*B*a and DEM subtraction) for four periods (1962-2013, 1962-1995, 1995-2013 and 2009-2013).

109x86mm (300 x 300 DPI)

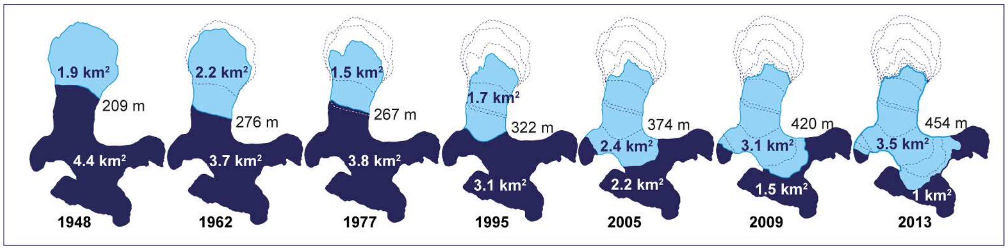

Figure 11: Elevation of the average 0°C-isotherm over AL for 7 years (1948, 1962, 1977, 1995, 2005, 2009 and 2013). The position of the 0°C isotherm elevation was estimated from the Ny-Ålesund temperature data of summer months (May-September) corrected from an elevation gradient of –0.005°C m^{-1}. The values in km^2 refer to the glacier area under (light blue) or over (dark blue) the 0°C-isotherm. The values in m are the elevation of the 0°C isotherm. Glacier elevation for 1948 and 1977 is that of 1962 and for 2005 it is that of 2009.

206x50mm (300 x 300 DPI)

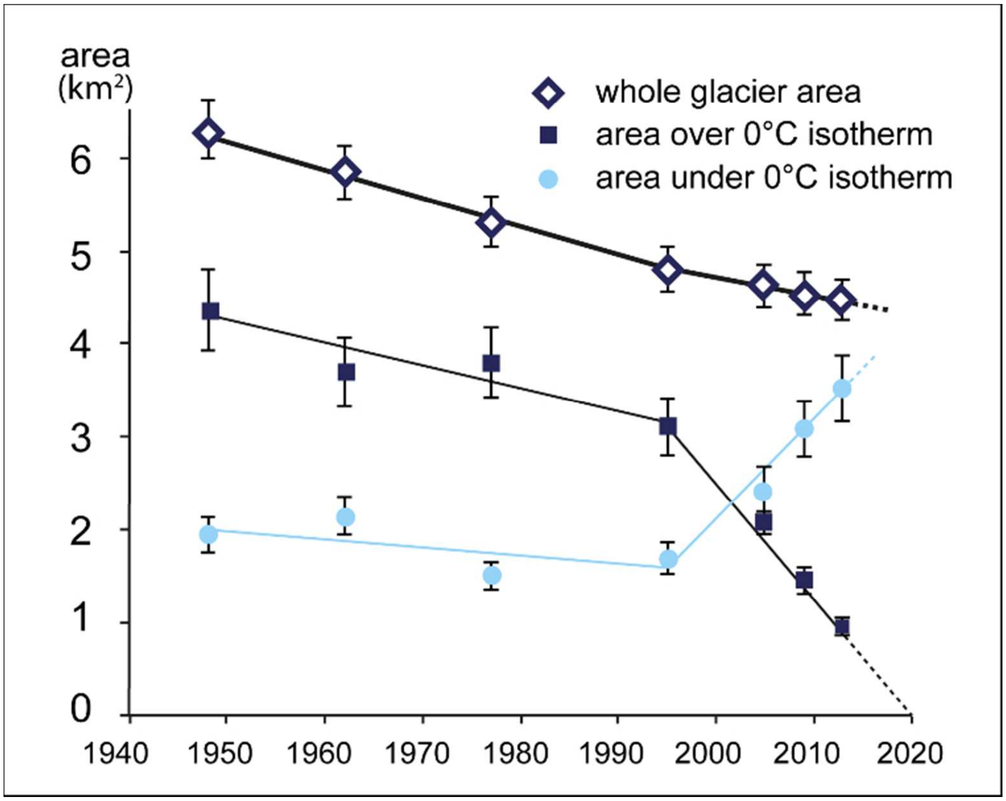

Figure 12: Areas (total, over and under 0°C isotherm) as a function of time (1948-2013).

64x50mm (300 x 300 DPI)